Table 1 Oligonucleotides used in the present study

	Oligonucleotide	*Sequence of oligonucleotide (5′-3′)*
1	For 5′ region of 75 Å α-helical spacer (sense)	CTAGTTACAAGCTGGCCGACGAGGAGACGCGGGCACGGCTG TCCAAGGAGCTGCAGGCGGCGCAGGCCCGGCTGGGCGCGG ACATGGAGGACGTGTGC
2	For 5′ region of 75 Å α-helical spacer (antisense)	GGCCGCACACGTCCTCCATGTCCGCGCCCAGCCGGGCCTGC GCCGCCTGCAGCTCCTTGGACAGCCGTGCCCGCGTCTCCTC GTCGGCCAGCTTGTAA
3	For central region of 75 Å α-helical spacer (sense)	GGCCGCCTGGTGCAGTACCGCGGCGAGGTGCAGGCCATGCT CGGCCAGAGCACCGAGGAGCTGCGGGTGCGCCTCGCCTCCC ACCTGCGCAAGCTGCGTAAGCGGCTCG
4	For central region of 75 Å α-helical spacer (antisense)	TCGACGAGCCGCTTACGCAGCTTGCGCAGGTGGGAGGCGAG GCGCACCCGCAGCTCCTCGGTGCTCTGGCCGAGCATGGCCTG CACCTCGCCGCGGTACTGCACCAGGC
5	For 3′ region of 75 Å α-helical spacer (sense)	TCGAGATCCCAACCTATCTGAGCGAAGATGAACTGAAAGCC GCCGAAGCCGCCTTCAAACGCCACAACCCAACCGCGTTCGA AG
6	For 3′ region of 75 Å α-helical spacer (antisense)	GATCCTTCGAACGCGGTTGGGTTCTGGCGTTTGAAGGCGGCT TCGGCGGCTTTCAGTTCATCTTCGCTCAGATAGGTTGGGATC
7	For restriction enzyme sites from *Asc*I to *Xba*I at the downstream of 75 Å α-helical spacer of pHM15-75 A (sense)	AATTGGCGCGCCGCGGCCGCGTAAATGAATAGACTAGTGCTA GCCCTAGGTCTAGAGTGC
8	For restriction enzyme sites from *Asc*I to *Xba*I at the downstream of 75 Å α-helical spacer of pHM15-75 A (antisense)	TCTAGACCTAGGGCTAGCACTAGTCTATTCATTTACGCGGCCG CGGCGCGCC
9	For GS linker plus RGD-4C peptide into pHM15-75A (sense)	CGAGGGATCCGGTTCAGGGAGTGGCTCTTGTGACTGCCGCG GAGACTGTTTCTGCTAA
10	For GS linker plus RGD-4C peptide into pHM15-75A (antisense)	CGCGTTAGCAGAAACAGTCTCCGCGGCAGTCACAAGAGCCA CTCCCTGAACCGGATCCCT
11	For RGD-4C peptide into the C-terminus of pIX or HVR5 of hexon (sense)	CTAGGGGCAGCTGTGACTGCCGCGGAGACTGTTTCTGCGGCA GCC
12	For RGD-4C peptide into the C-terminus of pIX or HVR5 of hexon (antisense)	CTAGGGCTGCCGCAGAAACAGTCTCCGCGGCAGTCACAGCT GCCC
13	For FLAG tag sequence into the C-terminus of pIX or HVR5 of hexon (sense)	CTAGGGGCAGCGACTACAAGGACGATGATGACAAAGGCAG CC
14	For FLAG tag sequence into the C-terminus of pIX or HVR5 of hexon (antisense)	CTAGGGCTGCCTTTGTCATCATCGTCCTTGTAGTCGCTGCCC
15	For FLAG tag sequence into pHM15-75A (sense)	CGAGGGATCCGGTTCAGGGAGTGGCTCTGACTACAAGGACG ATGATGACAAATAA
16	For FLAG tag sequence into pHM15-75A (antisense)	CGCGTTATTTGTCATCATCGTCCTTGTAGTCAGAGCCACTCCC TGAACCGGATCCCT
17	For His tag sequence into the C-terminus of pIX (sense)	CTAGGGGCAGCCATCACCATCACCATCACGGCAGCC
18	For His tag sequence into the C-terminus of pIX (antisense)	CTAGGGCTGCCGTGATGGTGATGGTGATGGCTGCCC
19	For His tag sequence into pHM15-75A (sense)	CGAGGGATCCGGTTCAGGGAGTGGCTCTCATCACCATCACCA TCACTAA
20	For His tag sequence into pHM15-75A (antisense)	CGCGTTAGTGATGGTGATGGTGATGAGAGCCACTCCCTGAAC CGGATCCCT

than that of the fiber, the intensity of the band of Ad-FLAG(pIX)-L2 was weaker than that of Ad-FLAG(HI)-L2 and Ad-FLAG(C)-L2. This phenomenon is not due to impaired incorporation efficiency of the modified-pIX (at least the modified-pIX without the 75 Å α-helical spacer), because similar intensity of the pIX band was observed between Ad-FLAG(pIX)-L2 and Ad-L2 by Western blotting using anti-pIX antibody (kindly provided by Dr Keith N Leppard, Biological Sciences University of Warwick Coventry, UK)[27] (Figure 5b; will be described later). It remains unclear why the results of Figure 2 (anti-FLAG tag antibody) and Figure 5 (anti-pIX antibody) are different. The discrepancy might result from the property of each antibody. Anti-FLAG tag antibody is monoclonal, while anti-pIX antibody is polyclonal. These results suggested that the FLAG tag peptide was expressed as a fusion protein of the fiber, pIX or hexon.

Next, we examined by enzyme linked immunosorbent assay (ELISA) whether the FLAG tag peptide in each region was displayed on the virus surface (Figure 3). Purified viruses were incubated in carbonate-bicarbonate buffer (Sigma) and immobilized on a 96-well immunoplate (NALGE NUNC International, Tokyo, Japan) at 4°C. On the following day, wells were washed with phosphate buffered saline and blocked with Block Ace. Anti-FLAG tag monoclonal antibody (1:1000) diluted in Block Ace was bound to the immobilized virus and washed with phosphate-buffered saline containing 0.05% Tween20 (Polyxyethylene (20) Sorbitan Monolaurate; Wako Pure Chemical Industries Ltd, Osaka, Japan). Next, a secondary antibody (goat anti-mouse IgG HRP-linked antibody) diluted in Block Ace (1:1000) was bound to a mouse anti-FLAG tag antibody, and HRP was detected by TMB PEROXIDASE SUBSTRATE (MOSS Inc., Pasadena, ML, USA). Absorbance at 450–655 nm was measured by microplate reader. Ad-FLAG(HI)-L2, Ad-FLAG(C)-L2, Ad-FLAG(pIX)-L2 and Ad-FLAG(hexon)-L2 showed higher absorbance values than Ad-L2. Ad-FLAG(hexon)-L2 showed the highest absorbance values among all FLAG tag peptides displaying Ad vectors (Figure 3). The absorbance values were dependent on the copy number of the fusion protein on the

Table 2 Ad vectors used in the present study

Ad vectors	*Vector plasmids*	*Fiber*		*pIX*	*Hexon (HVR5)*
		HI loop	*C-terminus*		
Ad-L2	pAdHM4-L2	—	—	—	—
Ad-FLAG(HI)-L2	pAdHM41-FLAG(HI)-L2	DYKDDDDK	—	—	—
Ad-FLAG(C)-L2	pAdHM41-FLAG(C)-L2	—	$(GS)_4$DYKDDDDK	—	—
Ad-FLAG(pIX)-L2	pAdHM56-FLAG-L2	—	—	GSDYKDDDDKGS	—
Ad-FLAG(pIX/75)-L2	pAdHM56-FLAG75-L2	—	—	α-Helical linker plus $(GS)_4$DYKDDDDK	—
Ad-FLAG(hexon)-L2	pAdHM62-FLAG-L2	—	—	—	GSDYKDDDDKGS
Ad-His(pIX)-L2	pAdHM56-His-L2	—	—	GSHHHHHHGS	—
Ad-His(pIX/75)-L2	pAdHM56-His75-L2	—	—	α-Helical linker plus $(GS)_4$HHHHHH	—
Ad-RGD(HI)-L2	pAdHM15-RGD-L2	ACDCRGDCFCD	—	—	—
Ad-RGD(C)-L2	pAdHM41-RGD-L2	—	$(GS)_4$ACDCRGDCFCG	—	—
Ad-RGD(pIX)-L2	pAdHM56-RGD-L2	—	—	GSCDCRGDCFCGS	—
Ad-RGD(pIX/75)-L2	pAdHM56-RGD75-L2	—	—	α-helical linker plus $(GS)_4$CDCRGDCFC	—
Ad-RGD(hexon)-L2	pAdHM62-RGD-L2	—	—	—	GSCDCRGDCFCGS

Abbreviation: Ad, adenovirus.
Each modified Ad vector has additional amino-acids derived from unique restriction enzyme sites (*Csp*45I, *Cla*I or *Xba*I) in each region, but not be described here.

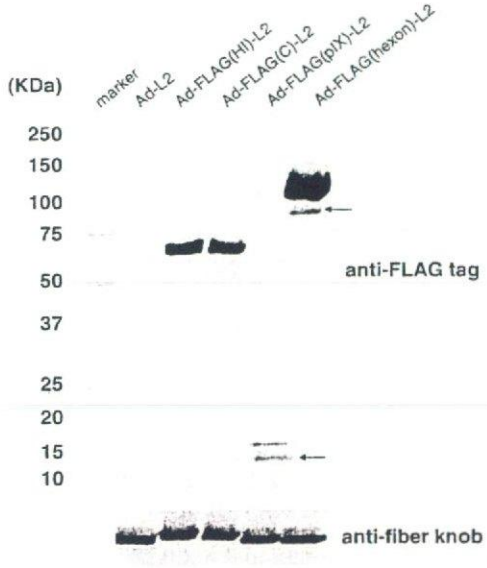

Figure 2 Western blotting of FLAG tag-modified Ad vectors. The total protein (1 μg) of each vector in 1 × sample buffer containing 4% β-mercaptoethanol was separated on a 4–20% SDS-PAGE gel, and the expression of the FLAG tag peptide was analyzed by Western blotting using mouse anti-FLAG tag monoclonal antibody. As a control, the membrane was also incubated with anti-fiber knob antibody (kindly provided by RD Gerard, University of Texas Southwestern Medical Center, Dallas, TX, USA). The band of the fiber of Ad-FLAG(HI)-L2 and Ad-FLAG(C)-L2 was higher than that of the other vectors, reflecting the insertion of the FLAG tag into the HI loop or C-terminus of the fiber knob. The extra bands marked with an arrow are proteolytic degradation products.

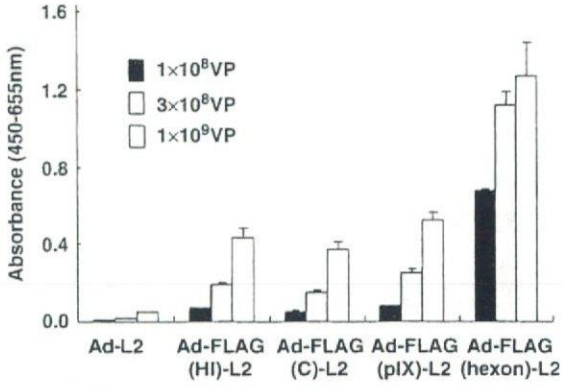

Figure 3 ELISA of FLAG tag-modified Ad vectors. Ad-L2, Ad-FLAG(HI)-L2, Ad-FLAG(C)-L2, Ad-FLAG(pIX)-L2 or Ad-FLAG(hexon)-L2 (10^9 VP/well, 3×10^8 VP/well, or 1×10^8 VP/well) were immobilized on a 96-well immunoplate. Mouse FLAG tag antibody was applied and then detected by anti-mouse IgG HRP-linked antibody. Absorbance at 450–655 nm was measured by microplate reader. The data are expressed as means ± s.d. ($n = 3$).

virus surface. Ad-FLAG(pIX)-L2, however, showed only slightly higher absorbance than Ad-FLAG(HI)-L2 and Ad-FLAG(C)-L2. ELISA is based on the ability of the anti-FLAG tag antibody to bind to the FLAG tag sequence on each Ad vector. The accessibility to the FLAG tag sequence at the C-terminus of pIX might be impaired, because pIX was buried between the hexon-tops. These results suggested that the fiber- (both the HI loop and C-terminus), pIX-, and the hexon-modified Ad vectors that were generated in this study did in fact display foreign ligands on the viral surface.

We and several groups have reported the feasibility of Ad vector application containing the RGD peptide in the HI loop or the C-terminus of the fiber knob, the C-terminus of pIX and the HVR5 region of the hexon.[9,10,18,21,28] However, there has been no report about which region is suitable for displaying the RGD peptide. To examine this, we constructed Ad vectors containing the RGD peptide in the fiber knob (HI loop or C-terminus), pIX (with or without 75 Å α-helical spacer),

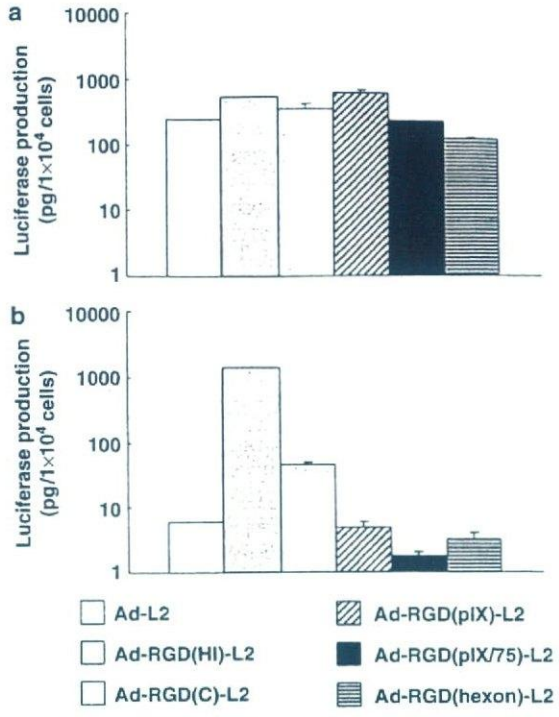

Figure 4 Transduction efficiency of RGD-modified Ad vectors. SK HEP-1 (**a**) and SF295 (**b**) cells were transduced with 3000 VP/cell of Ad-L2, Ad-RGD(HI)-L2, Ad-RGD(C)-L2, Ad-RGD(pIX)-L2, Ad-RGD(pIX/75A)-L2 or Ad-RGD(hexon)-L2 for 1.5 h, respectively. After culturing for 48 h, luciferase production was determined using a luciferase assay system (PicaGene LT2.0; Toyo Inki, Tokyo, Japan). The data are expressed as means ±s.d. ($n=3$).

and hexon and compared the luciferase production in SK HEP-1 and SF295 cells transduced with each vector (Figure 4). In the case of the pIX-modified Ad vector, the vector containing the 75 Å α-helical spacer between the C-terminus of pIX and the RGD peptide was also constructed as described previously,[18] together with the vector without the α-helical spacer. The RGD (CDCRGDCFC; RGD-4C) peptide binds to integrin αvβ3 and αvβ5 on the cellular surface.[29–31] SK HEP-1 cells were CAR-positive, while SF295 cells were CAR-negative. Both cells expressed αvβ3 and αvβ5 integrins (the expression of CAR and integrins in each cell was examined in our previous report by flow cytometry).[28] The luciferase enzymatic activity following transduction with Ad-RGD(HI)-L2, Ad-RGD(C)-L2, Ad-RGD(pIX)-L2, Ad-RGD(pIX/75)-L2 and Ad-RGD(hexon)-L2 was only about two to three times different from that with Ad-L2 in SK HEP-1 cells (Figure 4a). This would reflect that all vectors efficiently transduce via (at least) CAR. In contrast, in SF295 cells Ad-RGD(HI)-L2 and Ad-RGD(C)-L2 showed approximately 230- or 10-fold higher luciferase production, which mediated via an RGD-integrin-dependent pathway (our previous data and data not shown),[10,28] than Ad-L2 (Figure 4b). Luciferase production in SF295 cells transduced with Ad-RGD(pIX)-L2, Ad-RGD(pIX/75)-L2 and Ad-RGD(hexon)-L2 were not enhanced compared with Ad-L2. Lower luciferase production in SF295 cells transduced with Ad-RGD(hexon)-L2 was due to the about four times lower ratio of infectious titer-to-particle titer of Ad-RGD(hexon)-L2 in comparison with that of Ad-L2. These results suggested that the HI loop of the fiber knob is the most suitable region for capsid modification at least in the case of the insertion of the RGD peptide.

Vellinga *et al.*[18] reported that Ad vectors containing the RGD peptide at the C-terminus of pIX with a 75 Å α-helical spacer could transduce more efficiently into CAR-negative Eoma cells than vectors with a 30 or 45 Å α-helical spacer or no spacer. In the present study, we used a similar α-helical spacer sequence to that used by Vellinga *et al.*,[18] but no enhanced transduction was observed. The level of gene expression of Ad-RGD(pIX/75)-L2 was approximately three times lower in the SF295 cells than Ad-L2. We speculated that the lower transduction efficiency of Ad-RGD(pIX/75)-L2 might be due to the decreased incorporation efficiency of pIX-spacer-RGD into Ad-RGD(pIX/75)-L2. Therefore, we examined the incorporation of pIX into virus particles by Western blotting using the anti-pIX antibody (Figure 5a). The data obtained suggested that the incorporation efficiency of pIX-spacer-RGD into Ad-RGD(pIX/75)-L2 was greatly decreased, and only a faint band (marked with an asterisk) was observed, while that of pIX-RGD into Ad-RGD(pIX)-L2 was similar to that into Ad-L2, a control virus (Figure 5a). Therefore, a longer spacer might hamper incorporation efficiency. This would be the reason why Ad-RGD(pIX/75)-L2 did not show increased transduction efficiency. To examine this phenomenon in more detail, the incorporation of modified-pIX with the FLAG tag or His tag (HHHHHH) peptide into each virus was examined instead of the RGD peptide (Figure 5b). Modified-pIX without the spacer (Ad-FLAG(pIX)-L2 and Ad-His(pIX)-L2) was similarly incorporated into the wild-type virus (Ad-L2), while that with the spacer (Ad-FLAG(pIX/75)-L2 and Ad-His(pIX/75)-L2) was severely impaired. When the vectors were over-loaded on the SDS-PAGE gel, the band of the RGD-, FLAG tag- or His tag-modified pIX with a longer spacer was observed. Therefore, incorporation efficiency of modified-pIX was not completely impaired (Figure 5c). The pIX-spacer-His tag peptide was more efficiently incorporated into Ad-His(pIX/75)-L2 than the pIX-spacer-FLAG into Ad-FLAG(pIX/75)-L2, suggesting that the kind of peptide inserted might affect the incorporation efficiency when the longer spacer sequence is used. Vellinga *et al.*[18] reported the generation of pIX-modified Ad vector with a longer spacer by co-transfection of vector plasmid lacking pIX coding region and the plasmid expresses a series of modified pIX. The incorporation efficiency of pIX with a longer spacer into virion was lower than that of conventional-pIX, although their efficiency was higher than that in the present study. Subtle differences in the linker sequence between pIX and the longer spacer or between the longer spacer and the RGD peptide might have caused this difference in results. Their group recently reported new method for generation of pIX-modified Ad vectors.[32] They created a series of helper cell lines producing modified-pIX with and without longer spacers. The incorporation efficiency of pIX with a longer spacer into virion generated by the method was similar to that of unmodified-pIX. They also showed that the heat-stability of pIX-modified Ad vector with a longer spacer was worse than that of the

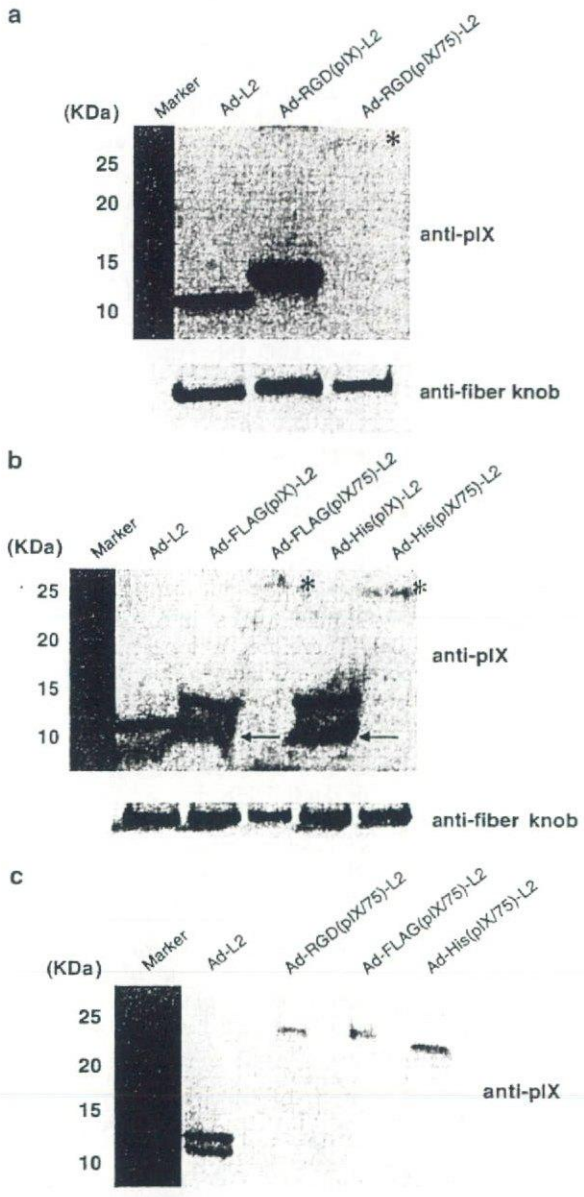

Figure 5 Analysis of the incorporation efficiency of modified-pIX. Incorporation efficiency of modified-pIX into the virus particles was determined by Western blotting. The total protein (**a** and **b**, 1 μg; **c**, 10 μg) of each vector in 1 × sample buffer containing 4% β-mercaptoethanol was separated on a 4–20% SDS-PAGE gel, and pIX was detected by the anti-pIX antibody. As a control, the anti-fiber knob antibody was used. (**a**) pIX-modified Ad vector containing the RGD peptide with or without a 75 Å α-helical spacer. (**b**) pIX-modified Ad vector containing the FLAG tag or His tag peptide with or without a 75 Å α-helical spacer. Ad-FLAG(pIX/75)-L2, Ad-His(pIX)-L2 and Ad-His(pIX/75)-L2 containing the FLAG tag or His tag peptide in the C-terminus of the pIX with or without a 75 Å α-helical spacer were similarly generated, as shown in Figure 1a. (**c**) The pIX-modifed Ad vector containing the RGD, FLAG tag, or His tag peptide with a 75 Å α-helical spacer. The extra bands marked with an arrow are proteolytic degradation products. The asterisks indicate the band of the modified-pIX with a 75 Å α-helical spacer.

conventional Ad vector and pIX-modified Ad vector without longer spacer. For these reasons, care should be taken in the use of a longer spacer.

Vigne *et al.*[21] have reported that Ad vectors containing the RGD peptide (DCRGDCF) at the HVR5 region of the hexon can infect cells via cellular αv integrin independently of CAR, which was inconsistent with the present study. The precise mechanism for these differences remains unclear. Subtle differences in the inserted RGD peptide sequence (SRGSCDCRGDCFCGSPR including the restriction enzyme-coding sequence in our study and GSDCRGDCFGS in their study) or the difference in the cell types used might have caused the discrepancy in results.

After we submitted this manuscript, Campos and Barry[33] reported a similar study in which fiber-, pIX- and hexon-modification were compared. They generated metabolically biotinylated Ad vectors by the insertion of the biotin acceptor peptide (BAP) in each location to directly compare targeted transduction through the fiber, pIX and hexon using a variety of biotinylated ligands, such as antibodies and proteins, which had a higher affinity than the RGD peptide. They reported that the modification of the fiber was more efficient than that of pIX and hexon,[33] which is consistent with the present report. They discussed how high affinity ligands at pIX or hexon made it impossible for the virus to escape from the endosome, and enter the cytoplasm, and traffic to the nucleus because the interaction between ligands at pIX or hexon and the cellular receptor was very strong. In the present study, we chose the RGD peptide to change (or expand) the tropism of the Ad vector, which had a lower affinity than antibodies or proteins. The modification of pIX and hexon with the RGD peptide might also have affected intracellular trafficking.

One of the possible reasons why the HI loop of the fiber knob is efficient in the case of the RGD peptide is that peptides displayed in the fiber knob can easily access the target molecules (receptors) because fiber knobs are the outmost capsid proteins of Ad vectors (the HI loop of the fiber knob is more exposed than the C-terminus). Therefore, pIX-modified or hexon-modified Ad vectors without the fiber proteins might show efficient ligand-mediated transduction because the ligand can come close to the cellular surface receptor. In addition, fiber-less Ad vectors do not infect cells via CAR due to the lack of fiber proteins.[34,35] pIX-modified or hexon-modified Ad vectors without fiber proteins could be a platform vector for targeting, although the fiber-less Ad vector was weaker against physical burdens, such as heat-treatment and freeze-and-thaw, than the conventional Ad vector (our unpublished data).

In summary, we have developed a simple method based on *in vitro* ligation to construct Ad vectors containing heterologous peptides in the C-terminus of pIX or the HVR5 region of the hexon. These Ad vectors displayed foreign peptides on the viral surface in each region. In the case of the insertion of the RGD peptide, Ad vectors modified in the HI loop of the fiber knob proved the better choice. As the vector system shown here enables easy construction of capsid-modified Ad vectors displaying a peptide of interest, it has great potential for gene therapy and gene transfer experiments.

Acknowledgements

The author thanks Tomomi Sasaki for technical assistance. This work was supported by grants from the

Ministry of Health, Labor, and Welfare of Japan. NK is the recipient of a fellowship from the Japan Society for the Promotion of Science.

References

1 Kovesdi I, Brough DE, Bruder JT, Wickham TJ. Adenoviral vectors for gene transfer. *Curr Opin Biotechnol* 1997; **8**: 583–589.
2 Benihoud K, Yeh P, Perricaudet M. Adenovirus vectors for gene delivery. *Curr Opin Biotechnol* 1999; **10**: 440–447.
3 Wickham TJ. Targeting adenovirus. *Gene Therapy* 2000; **7**: 110–114.
4 Mizuguchi H, Hayakawa T. Targeted adenovirus vectors. *Hum Gene Ther* 2004; **15**: 1034–1044.
5 Bergelson JM, Cunningham JA, Droguett G, Kurt-Jones EA, Krithivas A, Hong JS *et al*. Isolation of a common receptor for Coxsackie B viruses and adenoviruses 2 and 5. *Science* 1997; **275**: 1320–1323.
6 Tomko RP, Xu R, Philipson L. HCAR and MCAR: the human and mouse cellular receptors for subgroup C adenoviruses and group B coxsackieviruses. *Proc Natl Acad Sci USA* 1997; **94**: 3352–3356.
7 Dmitriev I, Krasnykh V, Miller CR, Wang M, Kashentseva E, Mikheeva G *et al*. An adenovirus vector with genetically modified fibers demonstrates expanded tropism via utilization of a coxsackievirus and adenovirus receptor-independent cell entry mechanism. *J Virol* 1998; **72**: 9706–9713.
8 Staba MJ, Wickham TJ, Kovesdi I, Hallahan DE. Modifications of the fiber in adenovirus vectors increase tropism for malignant glioma models. *Cancer Gene Ther* 2000; **7**: 13–19.
9 Mizuguchi H, Koizumi N, Hosono T, Utoguchi N, Watanabe Y, Kay MA *et al*. A simplified system for constructing recombinant adenoviral vectors containing heterologous peptides in the HI loop of their fiber knob. *Gene Therapy* 2001; **8**: 730–735.
10 Koizumi N, Mizuguchi H, Utoguchi N, Watanabe Y, Hayakawa T. Generation of fiber-modified adenovirus vectors containing heterologous peptides in both the HI loop and C terminus of the fiber knob. *J Gene Med* 2003; **5**: 267–276.
11 Dmitriev IP, Kashentseva EA, Curiel DT. Engineering of adenovirus vectors containing heterologous peptide sequences in the C terminus of capsid protein IX. *J Virol* 2002; **76**: 6893–6899.
12 Ghosh-Choudhury G, Haj-Ahmad Y, Graham FL. Protein IX, a minor component of the human adenovirus capsid, is essential for the packaging of full length genomes. *EMBO J* 1987; **6**: 1733–1739.
13 Furcinitti PS, van Oostrum J, Burnett RM. Adenovirus polypeptide IX revealed as capsid cement by difference images from electron microscopy and crystallography. *EMBO J* 1989; **8**: 3563–3570.
14 Rosa-Calatrava M, Grave L, Puvion-Dutilleul F, Chatton B, Kedinger C. Functional analysis of adenovirus protein IX identifies domains involved in capsid stability, transcriptional activity, and nuclear reorganization. *J Virol* 2001; **75**: 7131–7141.
15 Le LP, Everts M, Dmitriev IP, Davydova JG, Yamamoto M, Curiel DT. Fluorescently labeled adenovirus with pIX-EGFP for vector detection. *Mol Imag* 2004; **3**: 105–116.
16 Meulenbroek RA, Sargent KL, Lunde J, Jasmin BJ, Parks RJ. Use of adenovirus protein IX (pIX) to display large polypeptides on the virion–generation of fluorescent virus through the incorporation of pIX-GFP. *Mol Ther* 2004; **9**: 617–624.
17 Li J, Le L, Sibley DA, Mathis JM, Curiel DT. Genetic incorporation of HSV-1 thymidine kinase into the adenovirus protein IX for functional display on the virion. *Virology* 2005; **338**: 247–258.
18 Vellinga J, Rabelink MJ, Cramer SJ, van den Wollenberg DJ, Van der Meulen H, Leppard KN *et al*. Spacers increase the accessibility of peptide ligands linked to the carboxyl terminus of adenovirus minor capsid protein IX. *J Virol* 2004; **78**: 3470–3479.
19 Sumida SM, Truitt DM, Lemckert AA, Vogels R, Custers JH, Addo MM *et al*. Neutralizing antibodies to adenovirus serotype 5 vaccine vectors are directed primarily against the adenovirus hexon protein. *J Immunol* 2005; **174**: 7179–7185.
20 Roberts DM, Nanda A, Havenga MJ, Abbink P, Lynch DM, Ewald BA *et al*. Hexon-chimaeric adenovirus serotype 5 vectors circumvent pre-existing anti-vector immunity. *Nature* 2006; **441**: 239–243.
21 Vigne E, Mahfouz I, Dedieu JF, Brie A, Perricaudet M, Yeh P. RGD inclusion in the hexon monomer provides adenovirus type 5-based vectors with a fiber knob-independent pathway for infection. *J Virol* 1999; **73**: 5156–5161.
22 Wu H, Han T, Belousova N, Krasnykh V, Kashentseva E, Dmitriev I *et al*. Identification of sites in adenovirus hexon for foreign peptide incorporation. *J Virol* 2005; **79**: 3382–3390.
23 Mizuguchi H, Kay MA. A simple method for constructing E1- and E1/E4-deleted recombinant adenoviral vectors. *Hum Gene Ther* 1999; **10**: 2013–2017.
24 Mizuguchi H, Kay MA. Efficient construction of a recombinant adenovirus vector by an improved in vitro ligation method. *Hum Gene Ther* 1998; **9**: 2577–2583.
25 Mizuguchi H, Xu ZL, Sakurai F, Mayumi T, Hayakawa T. Tight positive regulation of transgene expression by a single adenovirus vector containing the rtTA and tTS expression cassettes in separate genome regions. *Hum Gene Ther* 2003; **14**: 1265–1277.
26 Maizel Jr JV, White DO, Scharff MD. The polypeptides of adenovirus. I. Evidence for multiple protein components in the virion and a comparison of types 2, 7A, and 12. *Virology* 1968; **36**: 115–125.
27 Caravokyri C, Leppard KN. Constitutive episomal expression of polypeptide IX (pIX) in a 293-based cell line complements the deficiency of pIX mutant adenovirus type 5. *J Virol* 1995; **69**: 6627–6633.
28 Koizumi N, Mizuguchi H, Hosono T, Ishii-Watabe A, Uchida E, Utoguchi N *et al*. Efficient gene transfer by fiber-mutant adenoviral vectors containing RGD peptide. *Biochim Biophys Acta* 2001; **1568**: 13–20.
29 Koivunen E, Wang B, Ruoslahti E. Phage libraries displaying cyclic peptides with different ring sizes: ligand specificities of the RGD-directed integrins. *Biotechnology (New York)* 1995; **13**: 265–270.
30 Pasqualini R, Koivunen E, Ruoslahti E. Alpha v integrins as receptors for tumor targeting by circulating ligands. *Nat Biotechnol* 1997; **15**: 542–546.
31 Arap W, Pasqualini R, Ruoslahti E. Cancer treatment by targeted drug delivery to tumor vasculature in a mouse model. *Science* 1998; **279**: 377–380.
32 Vellinga J, Uil TG, de Vrij J, Rabelink MJ, Lindholm L, Hoeben RC. A system for efficient generation of adenovirus protein IX-producing helper cell lines. *J Gene Med* 2006; **8**: 147–154.
33 Campos SK, Barry MA. Comparison of adenovirus fiber, protein IX, and hexon capsomeres as scaffolds for vector purification and cell targeting. *Virology* 2006; **349**: 453–462.
34 Legrand V, Spehner D, Schlesinger Y, Settelen N, Pavirani A, Mehtali M. Fiberless recombinant adenoviruses: virus maturation and infectivity in the absence of fiber. *J Virol* 1999; **73**: 907–919.
35 Von Seggern DJ, Chiu CY, Fleck SK, Stewart PL, Nemerow GR. A helper-independent adenovirus vector with E1, E3, and fiber deleted: structure and infectivity of fiberless particles. *J Virol* 1999; **73**: 1601–1608.

Available online at www.sciencedirect.com
SCIENCE DIRECT®
Journal of Controlled Release 113 (2006) 271–278
journal of controlled release
www.elsevier.com/locate/jconrel
GENE DELIVERY

The short consensus repeats 1 and 2, not the cytoplasmic domain, of human CD46 are crucial for infection of subgroup B adenovirus serotype 35

Fuminori Sakurai [a], Sayaka Murakami [a,b], Kenji Kawabata [a], Naoki Okada [c], Akira Yamamoto [b], Tsukasa Seya [d], Takao Hayakawa [e], Hiroyuki Mizuguchi [a,c,*]

[a] Laboratory of Gene Transfer and Regulation, National Institute of Biomedical Innovation, Osaka, 567-0085, Japan
[b] Department of Biopharmaceutics, Kyoto Pharmaceutical University, Kyoto, 607-8414, Japan
[c] Graduate School of Pharmaceutical Sciences, Osaka University, Osaka, 565-0871, Japan
[d] Department of Microbiology and Immunology, Graduate School of Medicine, Hokkaido University, Sapporo, 060-8638, Japan
[e] Pharmaceuticals and Medical Devices Agency, Tokyo, 100-0013, Japan

Received 21 October 2005; accepted 8 May 2006
Available online 21 June 2006

Abstract

Human CD46 (membrane cofactor protein) has recently been identified to be an attachment receptor for subgroup B adenoviruses (Ads); however, the precise interaction between human CD46 and subgroup B Ads are just beginning to be understood. In this study, to characterize the interaction between human CD46 and subgroup B Ads, varieties of mutant CD46 were tested for their ability to act as a receptor for Ad serotype 35 (Ad35), which belongs to subgroup B. In addition, we determined Ad35 vector-mediated transgene expression and cellular uptake of Ad35 vectors in the presence of a set of anti-CD46 antibodies. Our data demonstrated that the short consensus repeats (SCRs) 1 and 2 in human CD46 are important for interaction with Ad35, whereas the cytoplasmic domain of human CD46 was found not to be required for the function as an Ad35 receptor. Rather, a complete deletion of the cytoplasmic domain of human CD46 increased the transduction efficiencies of Ad35 vectors. This information should help in elucidation of the mechanism of subgroup B Ad infection, as well in the improvement of the subgroup B Ad vectors.

Keywords: Adenovirus serotype 35 vector; CD46; Short consensus repeat; Cytoplasmic tail; Gene therapy

1. Introduction

Human adenoviruses (Ads) compose a large family of non-enveloped, double-stranded DNA viruses that are a significant cause of acute respiratory, gastrointestinal, and ocular infections in humans. So far, at least 51 serotype Ads have been identified and classified into six distinct subgroups (A–F) [1,2]. Among them, subgroup B is further subdivided into subspecies B1 and B2 on the basis of various biophysical and biochemical criteria. Among the 51 human Ad serotypes, the Ad vector most commonly used for gene transfer is composed of Ad serotype 5 (Ad5), which belongs to subgroup C. Ad5 vectors are very powerful and useful vehicles, but recent studies have revealed that they also have some disadvantages, such as high seroprevalence toward Ad5 in adult populations and low infection activity in cells lacking a primary receptor for Ad5, coxsackievirus and adenovirus receptor (CAR). On the other hand, subgroup B Ads have unique properties that are distinct from those of other subgroup Ads, and that are highly attractive features as a framework for alternative gene delivery vehicles. First, subgroup B Ads have been identified as having lower prevalence than the Ads of other subgroups. The seroprevalences toward most subgroup B Ads is less than 20% in healthy blood donors, while more than 70% of serum samples from healthy donors are positive for anti-Ad5 antibody [3]. This indicates that transduction with Ad vectors based on subgroup B is unlikely to be inhibited by preexisting anti-Ad antibodies. Second, subgroup B Ads utilize human CD46 (membrane cofactor protein) as a cellular receptor for infection [4,5], while other subgroup Ads recognize CAR. Human CD46 is ubiquitously expressed in human cells, suggesting that subgroup

* Corresponding author. Laboratory of Gene Transfer and Regulation, National Institute of Biomedical Innovation, 7-6-8 Asagi, Saito, Ibaragi-City, Osaka, 567-0085, Japan. Tel.: +81 72 641 9815; fax: +81 72 641 9816.
E-mail address: mizuguch@nibio.go.jp (H. Mizuguchi).

0168-3659/$ - see front matter © 2006 Elsevier B.V. All rights reserved.
doi:10.1016/j.jconrel.2006.05.007

B Ad vectors would have a broad tropism for human cells. We have previously developed an Ad vector composed of Ad serotype 35 (Ad35), which belongs to subgroup B [6,7], and have demonstrated that Ad35 vectors exhibit a wider tropism for human cells, including CAR-negative cells, than Ad5 vectors [7].

Human CD46 is a type I transmembrane glycoprotein expressed in almost all human cells, except for erythrocytes. Human CD46 is composed of four cysteine-rich short consensus repeats (SCRs), a serine–threonine–proline-rich (STP) region, a short region of unknown function, a hydrophobic transmembrane domain, and a carboxy-terminal cytoplasmic domain. Alternative splicing in the STP region and the cytoplasmic domain gives rise to four major isoforms of human CD46 (BC1, BC2, C1, and C2). All the isoforms function as cofactors for the plasma serine protease factor I by binding to the complement factors C3b and C4b deposited on self tissue [8,9]. By promoting the proteolytic degradation of these factors, these isoforms protect the cells from complement attack [10,11]. In addition to this function, human CD46 has been identified to be a receptor for several human pathogens: measles virus (MV), human herpesvirus 6 (HHV6), human subgroup B Ads, and two types of bacteria [4,5,12–15]. Among these pathogens, the interactions between human CD46 and MV, HHV6, and pathogenic *Neisseria* have been well studied. MV-binding residues are located on SCR1 and SCR2 [16,17], while SCR3 and 4 are essential for binding of HHV6 to human CD46 [18]. The cytoplasmic domain of CD46 is not required for infection of both MV and HHV6 [18,19]. However, it still remains unknown which domains in human CD46 play an important role in the interaction with subgroup B Ads. Elucidation of the interaction between subgroup B Ads and CD46 would lead to improvement of the Ad vectors that are composed of subgroup B Ads.

In this study, the transduction experiments with Ad35 vectors expressing luciferase were performed using cells expressing a variety of human CD46 mutants in order to map the domains which interact with Ad35. Furthermore, cells expressing wild-type CD46 were transduced with Ad35 vectors in the presence of monoclonal anti-human CD46 antibodies which recognize different SCRs of human CD46. Finally, involvement of the cytoplasmic domain of human CD46 with infection of Ad35 was evaluated.

2. Materials and methods

2.1 Cells and antibodies

Chinese hamster ovary (CHO) cells and CHO transformants stably expressing wild-type CD46, CD46 SCR deletion mutants [16], or cytoplasmic tail deletion mutants were grown in Ham's F-12 medium with 10% fetal bovine serum. Cytoplasmic tail deletion mutants (ΔCyt0 and ΔCyt6 mutants) were stable CHO transformants generated by the transfection of pcDNA-CD46ΔCyt0 and pcDNA-CD46ΔCyt6 (described below) into CHO cells and selection with hygromycin (GIBCO-BRE, Rockville, MD). Monoclonal antibodies against human CD46 SCR1, E4.3, MEM-258, and J4-48 were purchased from Pharmingen (San Diego, CA), Serotec Ltd. (Oxford, United Kingdom), and Immunotech (Marseille, France), respectively. SCR2-specific antibody M177 and SCR3-specific antibody M160 were described previously [20]. The monoclonal anti-CD46 antibodies used in this study and their recognition sites are listed on Table 1

2.2. Plasmids

The plasmid pcDNA-CD46C2, which contains the human CD46 C2 isoform gene, was constructed as follows. The cDNA of the human CD46 C2 isoform was amplified by PCR using the following primers: CD46-forward, 5′-ATG GAG CCT CCC GGC CGC CGC GAG TGT CCC-3′; CD46-reverse, 5′-CGC GGC CGC CTA TTC AGC CTC TCT GCT CTG CTG-3′. The PCR product was cloned into the *Pme*I site of pcDNA3.1-Hyg(+) (Invitrogen, Carlsbad, CA). The cDNA of the CD46 mutant lacking the cytoplasmic tail (amino acid residues 347–369) (CD46ΔCyt0) was prepared by PCR using the parent CD46 C2 cDNA as a template. The following primers were used for PCR: CD46-forward (described above); and CD46TM-reverse, 5′-GCG GCC GCT CAG TAC GGG ACA ACA CAA ATT ACT GCA AC-3′. The PCR product was cloned into the *Pme*I site of pcDNA3.1-Hyg(+), resulting in pcDNA-CD46ΔCyt0. The plasmid pcDNA-CD46ΔCyt6, which contains a human CD46 C2 isoform lacking a portion of the cytoplasmic domain (amino acid residues 352–369) (CD46ΔCyt6), was constructed in a similar manner using the following primers: CD46-forward (described above); and CD46TM6-reverse, 5′-GCG GCC GCT CAC CTC CTT TGA AGA TAT CTG TAC GGG AC-3′. The sequences of all the constructs were confirmed by DNA sequencing.

2.3. Flowcytometric analysis of CD46 expression

Several CHO cell transformants suspended in staining buffer (phosphate buffered saline (PBS) buffer containing 1% bovine serum albumin (BSA)) were incubated with mouse anti-human CD46 antibodies (E4.3, M177, and M160) for 1 h. Subsequently, the cells were reacted with phycoerythrin (PE)-labeled secondary anti-mouse IgG antibody (Pharmingen). After washing with the staining buffer, the stained cells (10^4 cells) were analyzed using a FACSCalibur and CellQuest software (Becton Dickinson, Tokyo, Japan). For evaluation of Ad35 vector-mediated downregulation of CD46, the CHO transformants were transduced with Ad35L at 3000 vector particles (VP)/cell for 1.5 h as described below. After a 1.5-h incubation, CD46 expression levels in the cells were measured using flowcytometry as described above.

Table 1
Monoclonal anti-CD46 antibodies used in this study

Anti-CD46 antibodies	Recognition domain
E4.3	SCR1
J4-48	SCR1
MEM-258	SCR1
M177	SCR2
M160	SCR3

2.4. Adenovirus vectors

Ad35 vectors expressing luciferase, Ad35L, were prepared by an improved ligation method as previously described [21]. Briefly, the luciferase-expressing Ad35 vector plasmid pAdMS4-CMVL2 was constructed by ligating I-*Ceu*I/PI-*Sce*I-digested pAdMS4 with I-*Ceu*I/PI-*Sce*I-digested pCMVL1 [22]. pAdMS4-CMVL2 was digested with *Sbf*I and the linearized DNA was transfected into VK10-9 cells (kindly provided by Dr. V. Krougliak) [23]. Ad35L were generated 10–14 days after transfection, amplified and purified as described previously [6,7]. Determination of virus particle titers was accomplished spectrophotometrically by the method of Maizel et al. [24].

2.5. Transduction experiments

CHO cells and CHO transformants stably expressing wild-type CD46 or CD46 mutants lacking SCRs or the cytoplasmic tail were seeded at 1×10^4 cells/well into a 96-well plate. On the following day, the cells were transduced with Ad35L at 3000 VP/cell for 1.5 h. Forty-eight hours later, luciferase productions in the cells were measured using a luciferase assay system (PicaGene LT2.0, Toyo Inki Co. Ltd., Tokyo, Japan).

For antibody blocking experiments, CHO transformant expressing CD46 C2 isoform, which was seeded at 1×10^4 cells/well in a 96-well plate the day before transduction, was preincubated with the medium containing anti-CD46 antibodies (E4.3, MEM-258, J4-48, M177, and M160) at the indicated concentrations at 4 °C for 1 h. Ad35L was then added at 3000 VP/cell and left for 1.5 h at 4 °C, after which the cells were washed and incubated at 37 °C. Luciferase productions in the cells were measured 48 h after transduction as described above.

2.6. Real-time quantitative PCR

CHO cells and CHO transformants were seeded at 1×10^5 cells/well into a 12-well plate. On the following day, the cells were transduced with Ad35L as described above. After a 48-h incubation, the cells were washed with PBS, harvested, and pelleted. Total DNA, including the Ad35 vector DNA, was extracted from the cells using a Tissue DNeasy Kit (Qiagen, Valencia, CA, USA). The quantitative real-time PCR was performed with 25 ng of sample DNA, 0.5 μM each primer, 0.16 μM TaqMan probe, and 25 μl of TaqMan universal PCR master mix (Applied Biosystems, Foster City, CA, USA) in a final volume of 50 μl using the ABI Prism 7000 sequence detection system (Applied Biosystems). The PCR was initially denatured at 95 °C for 10 min and then subjected to cycles of 95 °C for 15 s and 60 °C for 1 min. The reaction was carried out for 50 cycles. Primers for amplification were located in the pIX region of Ad35 genome. The sequences of the primers and probe used were as follows: forward, 5′-TGGATGGAAGACCC GTTCAA-3′; reverse, 5′-CGTCCAAAGGTGAAGAACTTA AAGT-3′; probe, 5′ FAM-CGCCAATTCTTCAACGCTGACC TATGC-TAMRA 3′. These sequences were designed using Primer Express software version 1.0 (Applied Biosystems), and it was confirmed that they amplified the products of desired size. The Ad35 vector plasmid pAdMS4 was used as a standard.

3. Results

3.1. Ad35 vector-mediated transduction on CHO transformants expressing CD46 deletion mutants

First, we examined which SCR domains of human CD46 (Fig. 1) are essential for infection of Ad35 using CHO transformants expressing CD46 deletion mutants [16]. Before the transduction experiments, CD46 expression levels and SCR deletion on CHO transformants were confirmed by flowcytometric analysis using anti-CD46 antibodies against each of the SCRs. We found the sufficient levels of CD46 mutant expression for all the clones (Fig. 2). The combined use of several anti-CD46 antibodies demonstrated that the corresponding SCR domains were properly deleted on the CHO transformants. Deletion of SCR4 on the ΔSCR4 mutant was confirmed by RT-PCR and DNA sequence, because the SCR4-specific antibody was not obtained (data not shown).

Next, transduction experiments with Ad35 vectors on CHO transformants were performed. Transduction with Ad35L in ΔSCR1 and ΔSCR2 mutants resulted in approximately 50% of the luciferase production obtained in CHO-CD46 cells, which express full-length CD46. The decreases in the transduction efficiencies in ΔSCR1 and ΔSCR2 mutants were similar. In contrast, the ΔSCR3 and ΔSCR4 mutants produced amounts of luciferase similar to those in CHO-CD46 cells after Ad35L transduction (Fig. 3). Real-time PCR analysis also demonstrated that the uptake of Ad35L was significantly reduced by 58% and by 45% in ΔSCR1 and ΔSCR2 mutants, respectively, compared with CHO-CD46 cells, in contrast, ΔSCR3 and ΔSCR4 mutants exhibited the levels of Ad35 vector uptake similar to CHO-CD46 cells (Fig. 4). These results suggested that SCR1 and 2 are involved with Ad35 infection.

3.2. Blocking of Ad35 vector infection by anti-CD46 antibodies

Next, to further examine which SCR domains in CD46 are used for Ad35 infection, several monoclonal antibodies recognizing

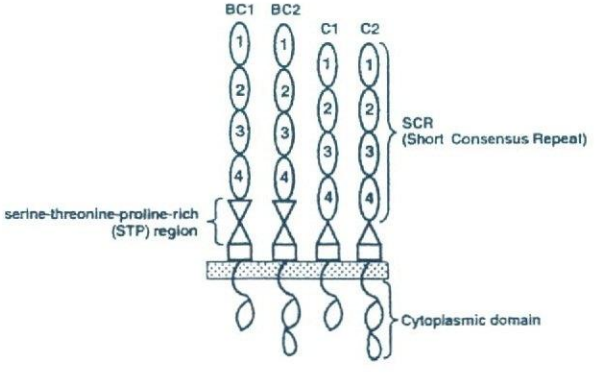

Fig. 1. A schematic diagram of human CD46. Human CD46 is ubiquitously expressed in almost all human cells mainly as four isoforms (BC1, BC2, C1, C2) that are derived via alternative splicing. Human CD46 is composed of four cysteine-rich short consensus repeats (SCRs), a serine–threonine–proline-rich (STP) region, a short region of unknown function, a hydrophobic transmembrane domain, and a carboxy-terminal cytoplasmic domain.

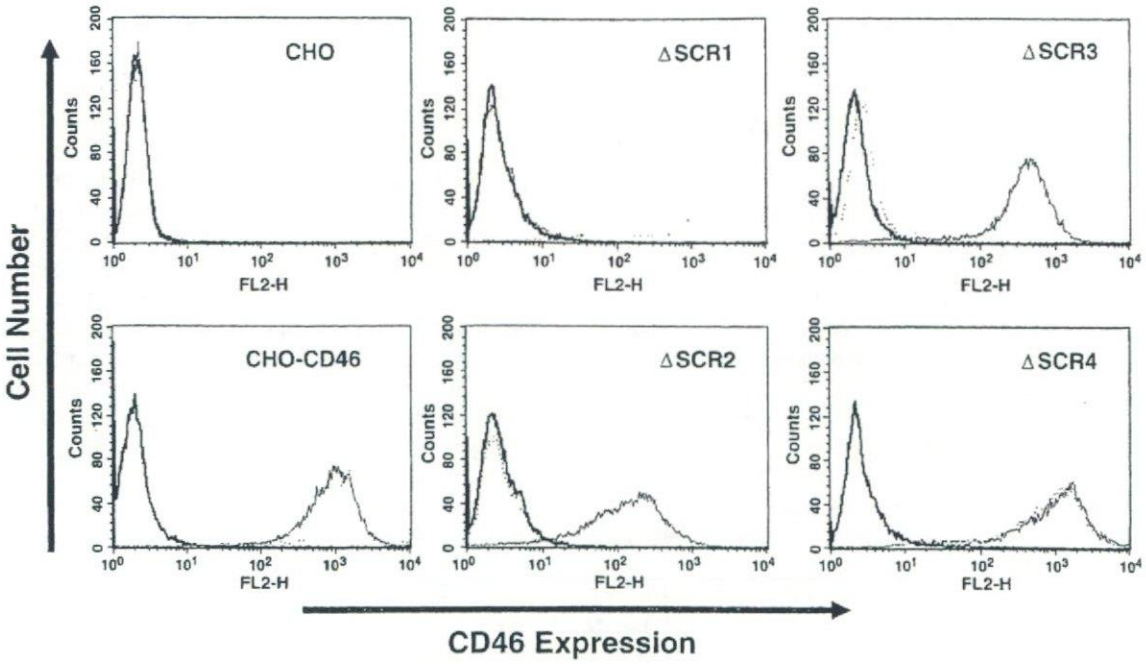

Fig. 2. Expression profiles of CD46 deletion mutants detected by monoclonal anti-CD46 antibodies. The cells were stained with anti-CD46 antibodies against SCR1 (E4.3; thin line), or SCR2 (M177; dotted line), followed by a PE-labeled secondary antibody, and subsequently analyzed by a flowcytometer. ΔSCR3 mutants were treated with anti-CD46 antibody against SCR3 (M160; dotted line) instead of M177. As a negative control, the cells were incubated with irrelevant control IgG, followed by a PE-labeled secondary antibody (thick line).

different domains of CD46 were used to block the transduction with Ad35 vectors. As shown in Fig. 5, the SCR1-specific antibody MEM-258 and the SCR2-specific antibody M177 efficiently inhibited the Ad35 vector-mediated transduction in CHO-CD46 cells. The manufacturer's information indicates that MEM-258 recognizes the SCR4 domain; however, our data indicates that MEM-258 binds to the SCR1 domain (data not shown). A recent study also reported that the epitope of MEM-258 is located in SCR1 [25]. We found that the luciferase production in the presence of both MEM-258 and M177 at 0.5 μg/ml was significantly reduced, compared with each of these antibodies alone (Fig. 5B). In contrast, the antibodies E4.3 and J4-48, which also recognize SCR1, did not decrease the luciferase production by Ad35L, suggesting that the region recognized by MEM-258, but not E4.3 and J4-48, would be involved with Ad35 infection. Decrease in the transduction efficiencies with Ad35L was not also found in the presence of the SCR3-specific antibody M160. The anti-CD46 antibodies which reduced the Ad35 vector-mediated transduction also inhibited the uptake of Ad35L by CHO-CD46 cells in a dose-dependent manner (Fig. 6). The SCR1-specific antibody MEM-258 and

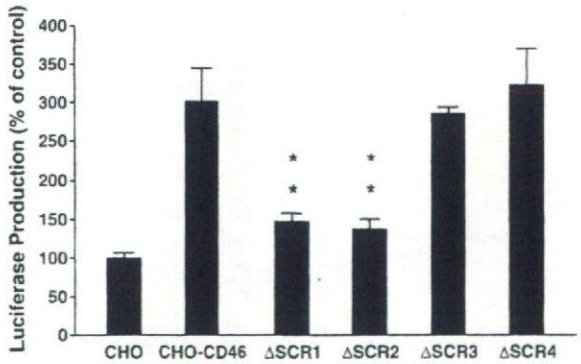

Fig. 3. Ad35L-mediated transduction in CHO cells expressing CD46 mutants lacking SCRs. The cells were transduced with Ad35L at 3000 VP/cell for 1.5 h. The luciferase productions in the cells were measured 48 h after transduction by luminescent assay. The data were normalized to the luciferase production in parental CHO cells. The absolute luciferase production in parental CHO cells was 200 pg/well. The data are expressed as the mean ± S.D. ($n=4$). The asterisks indicate the level of significance ($P<0.005$ [double asterisk] for comparison with CHO-CD46 cells).

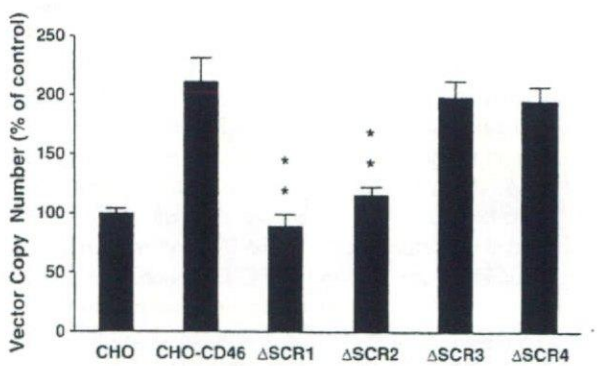

Fig. 4. Cellular uptake of Ad35L in CHO cells expressing CD46 mutants lacking SCRs. The cells were transduced with Ad35L at 3000 VP/cell for 1.5 h. The total DNA, including the vector DNA, was extracted from the cells 48 h after transduction. The copy numbers of the vector DNA were quantified by TaqMan-PCR. The data were normalized to the amounts of the vector DNA in CHO cells. The data are expressed as the mean ± S.D. ($n=3$). The asterisks indicate the level of significance ($P<0.005$ [double asterisk] for comparison with CHO-CD46 cells).

the SCR2-specific antibody M177 at 5 μg/ml decreased the cellular uptake of Ad35L by 94%. These results suggest that CD46 SCR1 and SCR2 are crucial domains for Ad35 infection.

3.3. Ad35 vector-mediated transduction on CHO cells expressing mutant CD46 lacking the cytoplasmic domain

To examine whether the intracellular domain of human CD46 is required for Ad35 infection, CHO transformants expressing human CD46 C2 isoforms lacking the cytoplasmic domain, CD46ΔCYT0 and CD46ΔCYT6, were transduced with Ad35L. All of the cytoplasmic domain is deleted in CD46ΔCYT0 (amino acid residues 347–369), while CD46ΔCYT6 contains the membrane-proximal 6 amino acids of the cytoplasmic tail and lacks a portion of the cytoplasmic domain (amino acid residues 352–369)

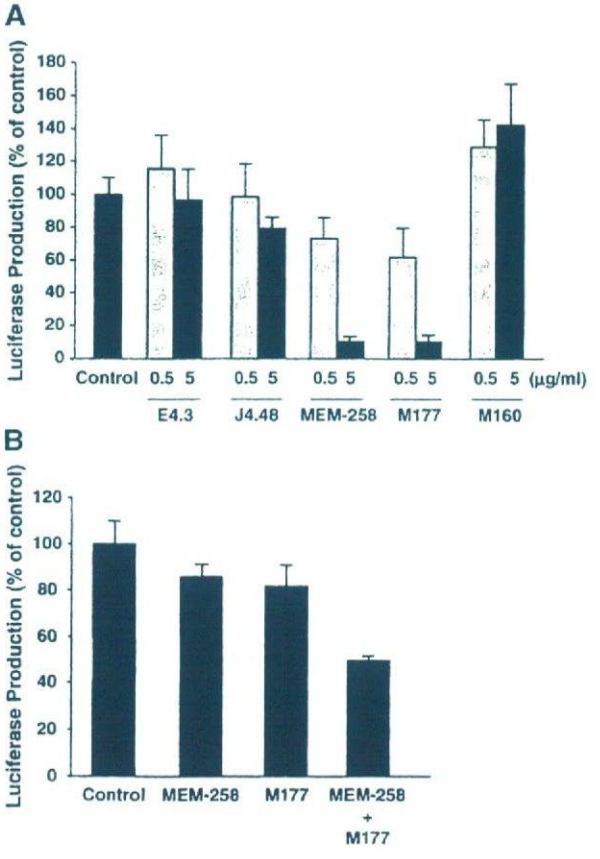

Fig. 5. Blocking of Ad35L-mediated transduction by monoclonal anti-CD46 antibodies. (A) Inhibition of Ad35L-mediated transduction by monoclonal anti-CD46 antibodies. E4.3, MEM-258, and J4-48 (recognizing SCR1), M177 (recognizing SCR2), and M160 (recognizing SCR3) were used as monoclonal anti-CD46 antibodies. CHO cells expressing wild-type CD46 were preincubated with each antibody at the indicated concentrations for 1 h and then infected with Ad35L at 3000 VP/cell. The luciferase productions in the cells were measured by luminescent assay 48 h after transduction. In control settings (Control), the cells were preincubated with medium only prior to transduction. The level of the luciferase production in control settings was almost the same as that in the presence of control mouse IgG (data not shown). (B) Combined inhibitory effect of MEM-258 and M177. The cells were preincubated with MEM-258 and/or M177 at 0.5 μg/ml. The transduction experiments were performed as described above. The data are expressed as the mean ± S.D. ($n=4$).

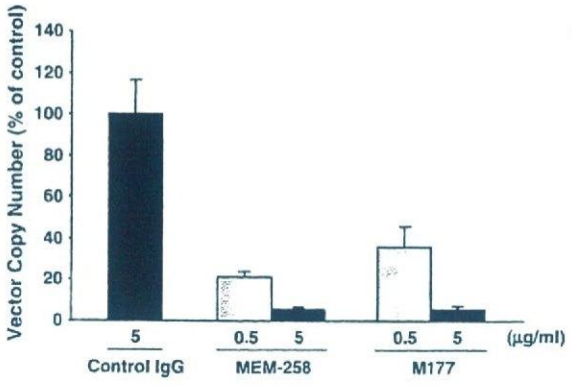

Fig. 6. Inhibition of cellular uptake of Ad35L by monoclonal anti-CD46 antibodies. CHO transformants expressing full-length CD46 were transduced with Ad35L in the presence of anti-CD46 antibody MEM-258 and M177 as described in Fig. 5. The total DNA, including the vector DNA, was extracted 48 h after transduction. The vector copy number was quantified by TaqMan-PCR. The data were normalized to the amounts of the vector DNA in CHO cells expressing full-length CD46 in the presence of control mouse IgG. The data are expressed as the mean ± S.D. ($n=4$).

including the potential phosphorylation domain [26,27], which might be involved with various intracellular events, such as Ca^{2+} flux. The efficiency of the Ad35L-mediated transduction was similar between CHO cells expressing CD46ΔCYT6 and CHO cells expressing the full-length CD46 (Fig. 7). Furthermore, deletion of all the cytoplasmic domain significantly increased the transduction efficiency with Ad35L. These results indicate that the cytoplasmic domain of human CD46 would not be required to serve as a receptor for Ad35.

Next, we further measured the levels of CD46 expression in CHO transformants expressing wild-type CD46 or CD46ΔCYT0 following transduction with Ad35L to investigate why deletion of all the cytoplasmic domain increased the Ad35 vector-mediated transduction efficiency. The cytoplasmic domain is largely responsible to the downregulation of CD46 induced by MV [28], and

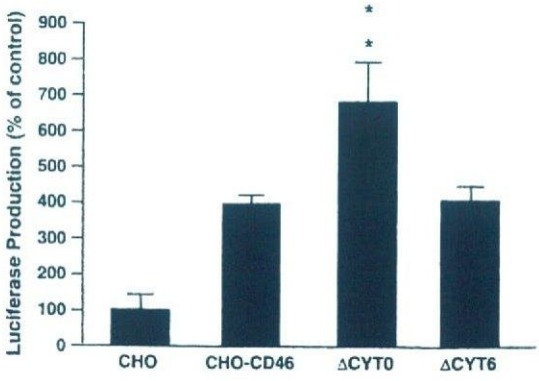

Fig. 7. Ad35L-mediated transduction in CHO cells expressing CD46 mutants lacking the cytoplasmic domain. The cells were transduced with Ad35L at 3000 VP/cells for 1.5 h. The luciferase productions in the cells were measured 48 h after transduction by luminescent assay. The data were normalized to the luciferase production in parental CHO cells. The data are expressed as the mean ± S.D. ($n=4$). The asterisks indicate the level of significance ($P<0.005$ [double asterisk] for comparison with CHO-CD46).

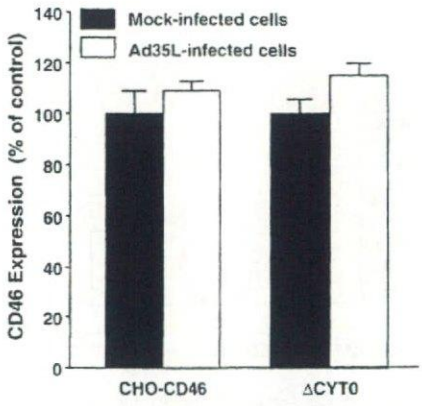

Fig. 8. CD46 expression levels in CHO transformants after infection with Ad35L. The CHO transformants expressing full-length CD46 or CD46ΔCYT0 were transduced with Ad35L at 3000 VP/cell for 1.5 h. After a 1.5-h incubation, the cells were subjected to flowcytometric analysis for measurement of CD46 expression. The data are expressed as the mean ± S.D. ($n=4$).

CD46 downregulation might influence the infectivity of the viruses. Flowcytometric analysis demonstrated that CD46 downregulation did not occur in both CHO transformants expressing full-length CD46 or CD46ΔCYT0 following transduction with Ad35L (Fig. 8), suggesting that CD46 downregulation by Ad35 vectors was not involved in the increase in the transduction efficiencies of Ad35L in CHO cells expressing CD46ΔCYT0.

4. Discussion

Elucidation of the interaction between viruses and their receptors is of great importance for studies of virus pathogenicity. In addition, for the viruses that provide a framework for gene delivery vehicles, such information may help us not only to evaluate the transduction properties of virus vectors but also to improve virus vectors. In this study, CHO cells expressing CD46 deletion mutants and several monoclonal anti-CD46 antibodies were used to examine which regions are crucial for Ad35 infection. Infection experiments in cells expressing CD46 mutants lacking SCRs and blocking experiments using monoclonal anti-CD46 antibodies have already been used to determine the essential regions for infection of the pathogens recognizing CD46 in previous studies [16–18,29]. We applied this approach to elucidation of the crucial regions in CD46 for subgroup B Ad infection. The results presented herein demonstrated that the essential domains for Ad35 infection are located in SCR1 and 2, and that deletion of all the cytoplasmic domain in CD46 significantly increases Ad35 vector-mediated transduction.

Previous studies have demonstrated that MV binds to SCR1 and 2 [16,17], whereas infection of HHV6 is mediated by SCR2 and 3 [18]. Thus, SCR2 of CD46 is a crucial domain for all the human viruses utilizing CD46 (MV, HHV6, and subgroup B Ads). Moreover, SCR2-specific antibody M177 significantly inhibits the infection of all three viruses (Fig. 3) [18], suggesting that these viruses would interact with the region recognized by M177. The amino acids important for M177 binding, R69 and D70, which are located in the middle of SCR2 [30], are also present in CD46 of the cynomolgus monkey [31], which is susceptible to MV and HHV6. We also confirmed that primary cells isolated from the cynomolgus monkey were efficiently transduced with Ad35 vectors (data not shown).

Deletion of SCR1 as well as SCR2 largely decreased both the transduction efficiency and the cellular uptake of Ad35L (Figs. 3 and 4). However, SCR1-specific E4.3 and J4-48 did not significantly reduce the luciferase productions by Ad35L (Fig. 5). On the other hand, the antibody MEM-258, which also recognizes SCR1, significantly inhibited the Ad35 vector-mediated transduction and cellular uptake of Ad35L (Figs. 5 and 6). The amino acids important for binding of E4.3 and J4-48 are located on the top of SCR1 [31]. At present, it remains unclear where the epitope of MEM-258 is located within SCR1; however, the location of the epitope of MEM-258 would be different from those of E4.3 and J4-48, and would be important for Ad35 infection.

Recognition of SCR1 and 2 by Ad35 would be favorable for infection of Ad35. SCR1 and 2 are located on the upper region of CD46, leading to the decrease in electrostatic repulsion between the virus capsid and acidic cell surface proteins and the increase in attachment of Ad35 to the cell surface. Shayakhmetov and Lieber demonstrated that electrostatic repulsion between the virus capsid and cell surface is an important factor for Ad infection, especially for Ads possessing a short fiber shaft [32]. Ad35 has a shorter fiber shaft (9 nm) than Ad5 (37 nm).

During the preparation of this manuscript, two reports concerning the domains of human CD46 which interact with subgroup B Ads were published [25,33]. Gaggar et al. demonstrated that the subgroup B Ad-binding domain is located within SCR2 alone [33], while Fleischli et al. reported that the presence of both SCR1 and 2 is sufficient for infection of Ad35 and that binding of Ad35 is not confined to a single SCR domain [25]. Our data support the conclusion of Fleischli et al. The SCR2-specific antibody M177 and the deletion of SCR2 decreased Ad35 vector-mediated transduction (Figs. 3–6), suggesting that the region in SCR2 recognized by M177 would be important for interaction with Ad35. Luciferase production by Ad35L and cellular uptake of Ad35L in ΔSCR1 mutants was largely decreased, compared with CHO-CD46 cells (Figs. 3 and 4), suggesting that SCR1 would also play a role in Ad35 infection. Although the decrease in luciferase production and cellular uptake of Ad35L in the ΔSCR1 mutant might be due to conformational change of SCR2 by the deletion of SCR1, this is unlikely because the SCR2-specific antibody M177 showed positive staining in the ΔSCR1 mutant (Fig. 2). This suggests that the region recognized by M177 would hold an appropriate conformation in the ΔSCR1 mutant. Therefore, we conclude that both SCR1 and SCR2 are involved with Ad35 infection. The finding that the SCR1-specific antibody MEM-258 largely inhibited the transduction with Ad35L supports this conclusion (Figs. 5 and 6).

The cytoplasmic domain of human CD46 is not an absolute requirement in order for this protein to serve as an attachment receptor for Ad35 (Fig. 7). MV and HHV6 can also infect cells via mutant CD46 lacking the cytoplasmic domain [18,19]. However, the luciferase production was significantly increased in ΔCYT0, compared with that in CHO-CD46, in contrast, Ad35L mediated similar levels of luciferase productions in both CHO-CD46 and ΔCYT6. It remains unclear why the deletion of

the entire cytoplasmic domain of human CD46 increased the transduction efficiency, however, downregulation of CD46 was not observed in both CHO-CD46 and ΔCYT0 after transduction with Ad35L (Fig. 7). These results suggest that the increase in the transduction efficiencies of Ad35L in ΔCYT0 was not due to the lack of CD46 downregulation. One possibility for the increased transduction efficiencies in ΔCYT0 is that the amounts of CD46 which Ad35 vectors can access to would be increased by the deletion of the cytoplasmic domain. Maisner et al. demonstrated that CD46 are predominantly distributed in basolateral side of the cells and that CD46 lacking the entire cytoplasmic domain were transported to both apical and basolateral sides [34]. CD46ΔCYT0 might be more widely distributed than full-length CD46 in the CHO transformants, leading to the increase in the infection of Ad35 vectors. Another possibility is that the membrane-proximal 6 amino acids of the cytoplasmic domain in CD46 C2 isoform might contain a signal sequence for suppression of viral infection. Mouse macrophages expressing a tailless human CD46 mutant are more susceptible to MV infection than those expressing wild-type CD46 [35]. In addition to these functions of the cytoplasmic domain, the cytoplasmic domain plays important roles in immune responses through CD46, such as cytokine productions. Hirano et al. reported that the production of high levels of NO and IL-12 upon MV infection is dependent on the CD46 cytoplasmic domain [35]. Kurita-Taniguchi et al. demonstrated that intracellular phosphatase SHP-1 was found to be recruited to the cytoplasmic tail of human CD46 when human macrophages became sufficiently mature to produce IL-12 and NO in response to measles virus [36]. Therefore, the cytoplasmic domain might be involved with immune responses induced by Ad35 infection.

In summary, we demonstrated here that SCR1 and 2 of human CD46 are required for Ad35 infection, while the cytoplasmic domain of human CD46 is not crucial for an attachment receptor function for Ad35. These results offer insight into the interaction between human CD46 and subgroup B Ads, such as the internalization of Ad35 into the cells via CD46 and the crucial domain in the Ad35 fiber knob for binding to CD46.

Acknowledgements

We would like to thank Dr. Yasuko Mori (Laboratory of Virology and Vaccinology, National Institute of Biomedical Innovation, Osaka, Japan) for her advice on the cell culture. This work was supported in part by a Grants-in-Aid for Scientific Research from the Ministry of Education, Culture, Sports, Science, and Technology of Japan, and by grants for Health and Labour Sciences Research from the Ministry of Health, Labour, and Welfare of Japan.

References

[1] M.J. Havenga, A.A. Lemckert, O.J. Ophorst, M. van Meijer, W.T. Germeraad, J. Grimbergen, M.A. van Den Doel, R. Vogels, J. van Deutekom, A.A. Janson, J.D. de Bruijn, F. Uytdehaag, P.H. Quax, T. Logtenberg, M. Mehtali, A. Bout, Exploiting the natural diversity in adenovirus tropism for therapy and prevention of disease, J. Virol. 76 (2002) 4612–4620.

[2] J.C. De Jong, A.G. Wermenbol, M.W. Verweij-Uijterwaal, K.W. Slaterus, P. Wertheim-Van Dillen, G.J. Van Doornum, S.H. Khoo, J.C. Hierholzer, Adenoviruses from human immunodeficiency virus-infected individuals, including two strains that represent new candidate serotypes Ad50 and Ad51 of species B1 and D, respectively, J. Clin. Microbiol. 37 (1999) 3940–3945.

[3] R. Vogels, D. Zuijdgeest, R. van Rijnsoever, E. Hartkoorn, I. Damen, M.P. de Bethune, S. Kostense, G. Penders, N. Helmus, W. Koudstaal, M. Cecchini, A. Wetterwald, M. Sprangers, A. Lemckert, O. Ophorst, B. Koel, M. van Meerendonk, P. Quax, L. Panitti, J. Grimbergen, A. Bout, J. Goudsmit, M. Havenga, Replication-deficient human adenovirus type 35 vectors for gene transfer and vaccination: efficient human cell infection and bypass of preexisting adenovirus immunity, J. Virol. 77 (2003) 8263–8271.

[4] A. Gaggar, D.M. Shayakhmetov, A. Lieber, CD46 is a cellular receptor for group B adenoviruses, Nat. Med. 9 (2003) 1408–1412.

[5] A. Segerman, J.P. Atkinson, M. Marttila, V. Dennerquist, G. Wadell, N. Arnberg, Adenovirus type 11 uses CD46 as a cellular receptor, J. Virol. 77 (2003) 9183–9191.

[6] F. Sakurai, H. Mizuguchi, T. Hayakawa, Efficient gene transfer into human CD34+ cells by an adenovirus type 35 vector, Gene Ther. 10 (2003) 1041–1048.

[7] F. Sakurai, H. Mizuguchi, T. Yamaguchi, T. Hayakawa, Characterization of in vitro and in vivo gene transfer properties of adenovirus serotype 35 vector, Mol. Ther. 8 (2003) 813–821.

[8] T. Seya, J.R. Turner, J.P. Atkinson, Purification and characterization of a membrane protein (gp45-70) that is a cofactor for cleavage of C3b and C4b, J. Exp. Med. 163 (1986) 837–855.

[9] T. Seya, J.P. Atkinson, Functional properties of membrane cofactor protein of complement, Biochem. J. 264 (1989) 581–588.

[10] T. Seya, T. Hara, M. Matsumoto, Y. Sugita, H. Akedo, Complement-mediated tumor cell damage induced by antibodies against membrane cofactor protein (MCP, CD46), J. Exp. Med. 172 (1990) 1673- 1680.

[11] D.M. Lublin, K.E. Coyne, Phospholipid-anchored and transmembrane versions of either decay-accelerating factor or membrane cofactor protein show equal efficiency in protection from complement-mediated cell damage, J. Exp. Med. 174 (1991) 35–44.

[12] F. Santoro, P.E. Kennedy, G. Locatelli, M.S. Malnati, E.A. Berger, P. Lusso, CD46 is a cellular receptor for human herpesvirus 6, Cell 99 (1999) 817–827.

[13] R.E. Dorig, A. Marcil, A. Chopra, C.D. Richardson, The human CD46 molecule is a receptor for measles virus (Edmonston strain), Cell 75 (1993) 295–305.

[14] H. Kallstrom, M.K. Liszewski, J.P. Atkinson, A.B. Jonsson, Membrane cofactor protein (MCP or CD46) is a cellular pilus receptor for pathogenic *Neisseria*, Mol. Microbiol. 25 (1997) 639–647.

[15] N. Okada, M.K. Liszewski, J.P. Atkinson, M. Caparon, Membrane cofactor protein (CD46) is a keratinocyte receptor for the M protein of the group A streptococcus, Proc. Natl. Acad. Sci. U. S. A. 92 (1995) 2489–2493.

[16] K. Iwata, T. Seya, Y. Yanagi, J.M. Pesando, P.M. Johnson, M. Okabe, S. Ueda, H. Ariga, S. Nagasawa, Diversity of sites for measles virus binding and for inactivation of complement C3b and C4b on membrane cofactor protein CD46, J. Biol. Chem. 270 (1995) 15148–15152.

[17] M. Manchester, A. Valsamakis, R. Kaufman, M.K. Liszewski, J. Alvarez, J.P. Atkinson, D.M. Lublin, M.B. Oldstone, Measles virus and C3 binding sites are distinct on membrane cofactor protein (CD46), Proc. Natl. Acad. Sci. U. S. A. 92 (1995) 2303–2307.

[18] H.L. Greenstone, F. Santoro, P. Lusso, E.A. Berger, Human herpesvirus 6 and measles virus employ distinct CD46 domains for receptor function, J. Biol. Chem. 277 (2002) 39112–39118.

[19] T. Seya, M. Kurita, K. Iwata, Y. Yanagi, K. Tanaka, K. Shida, M. Hatanaka, M. Matsumoto, S. Jun, A. Hirano, S. Ueda, S. Nagasawa, The CD46 transmembrane domain is required for efficient formation of measles-virus-mediated syncytium, Biochem. J. 322 (Pt 1) (1997) 135–144.

[20] T. Seya, T. Hara, M. Matsumoto, H. Akedo, Quantitative analysis of membrane cofactor protein (MCP) of complement. High expression of MCP on human leukemia cell lines, which is down-regulated during cell differentiation, J. Immunol. 145 (1990) 238–245.

[21] F. Sakurai, K. Kawabata, T. Yamaguchi, T. Hayakawa, H. Mizuguchi, Optimization of adenovirus serotype 35 vectors for efficient transduction in human hematopoietic progenitors: comparison of promoter activities, Gene Ther. 12 (2005) 1424–1433.

[22] H. Mizuguchi, N. Koizumi, T. Hosono, N. Utoguchi, Y. Watanabe, M.A. Kay, T. Hayakawa, A simplified system for constructing recombinant adenoviral vectors containing heterologous peptides in the H1 loop of their fiber knob, Gene Ther. 8 (2001) 730–735.

[23] V. Krougliak, F.L. Graham, Development of cell lines capable of complementing E1, E4, and protein IX defective adenovirus type 5 mutants, Hum. Gene Ther. 6 (1995) 1575–1586.

[24] J.V. Maizel Jr., D.O. White, M.D. Scharff, The polypeptides of adenovirus. I. Evidence for multiple protein components in the virion and a comparison of types 2, 7A, and 12, Virology 36 (1968) 115–125.

[25] C. Fleischli, S. Verhaagh, M. Havenga, D. Sirena, W. Schaffner, R. Cattaneo, U.F. Greber, S. Hemmi, The distal short consensus repeats 1 and 2 of the membrane cofactor protein CD46 and their distance from the cell membrane determine productive entry of species B adenovirus serotype 35, J. Virol. 79 (2005) 10013–10022.

[26] M.K. Liszewski, I. Tedja, J.P. Atkinson, Membrane cofactor protein (CD46) of complement. Processing differences related to alternatively spliced cytoplasmic domains, J. Biol. Chem. 269 (1994) 10776–10779.

[27] G. Wang, M.K. Liszewski, A.C. Chan, J.P. Atkinson, Membrane cofactor protein (MCP; CD46): isoform-specific tyrosine phosphorylation, J. Immunol. 164 (2000) 1839–1846.

[28] A. Hirano, S. Yant, K. Iwata, J. Korte-Sarfaty, T. Seya, S. Nagasawa, T.C. Wong, Human cell receptor CD46 is down regulated through recognition of a membrane-proximal region of the cytoplasmic domain in persistent measles virus infection, J. Virol. 70 (1996) 6929–6936.

[29] Y. Mori, T. Seya, H.L. Huang, P. Akkapaiboon, P. Dhepakson, K. Yamanishi, Human herpesvirus 6 variant A but not variant B induces fusion from without in a variety of human cells through a human herpesvirus 6 entry receptor, CD46, J. Virol. 76 (2002) 6750–6761

[30] C.J. Buchholz, D. Koller, P. Devaux, C. Mumenthaler, J. Schneider-Schaulies, W. Braun, D. Gerlier, R. Cattaneo, Mapping of the primary binding site of measles virus to its receptor CD46, J. Biol. Chem. 272 (1997) 22072–22079.

[31] E.C. Hsu, S. Sabatinos, F.J. Hoedemaeker, D.R. Rose, C.D. Richardson, Use of site-specific mutagenesis and monoclonal antibodies to map regions of CD46 that interact with measles virus H protein, Virology 258 (1999) 314–326.

[32] D.M. Shayakhmetov, A. Lieber, Dependence of adenovirus infectivity on length of the fiber shaft domain, J. Virol. 74 (2000) 10274–10286.

[33] A. Gaggar, D.M. Shayakhmetov, M.K. Liszewski, J.P. Atkinson, A. Lieber, Localization of regions in CD46 that interact with adenovirus, J. Virol. 79 (2005) 7503–7513.

[34] A. Maisner, M.K. Liszewski, J.P. Atkinson, R. Schwartz-Albiez, G. Herrler, Two different cytoplasmic tails direct isoforms of the membrane cofactor protein (CD46) to the basolateral surface of Madin–Darby canine kidney cells, J. Biol. Chem. 271 (1996) 18853–18858.

[35] A. Hirano, Z. Yang, Y. Katayama, J. Korte-Sarfaty, T.C. Wong, Human CD46 enhances nitric oxide production in mouse macrophages in response to measles virus infection in the presence of gamma interferon: dependence on the CD46 cytoplasmic domains, J. Virol. 73 (1999) 4776–4785.

[36] M. Kurita-Taniguchi, A. Fukui, K. Hazeki, A. Hirano, S. Tsuji, M. Matsumoto, M. Watanabe, S. Ueda, T. Seya, Functional modulation of human macrophages through CD46 (measles virus receptor): production of IL-12 p40 and nitric oxide in association with recruitment of protein-tyrosine phosphatase SHP-1 to CD46, J. Immunol. 165 (2000) 5143–5152.

Clinical immunology

Dendritic cells modified to express fractalkine/CX3CL1 in the treatment of preexisting tumors

Mio Nukiwa[*1], Sita Andarini*[*1], Jamal Zaini*[*1], Hong Xin[1,2], Masahiko Kanehira[1,2], Takuji Suzuki[1], Tatsuro Fukuhara[1], Hiroyuki Mizuguchi[3], Takao Hayakawa[4], Yasuo Saijo[1,2], Toshihiro Nukiwa[1] and Toshiaki Kikuchi[1]*

[1] Department of Respiratory Oncology and Molecular Medicine, Institute of Development, Aging and Cancer, Tohoku University, Sendai, Japan
[2] Department of Molecular Medicine, Tohoku University Graduate School of Medicine, Sendai, Japan
[3] Project III, National Institute of Health Sciences, Osaka Branch, Fundamental Research Laboratories for Development of Medicine, Osaka, Japan
[4] National Institute of Health Sciences, Tokyo, Japan

Received 29/9/05
Revised 26/12/06
Accepted 12/2/06

[DOI 10.1002/eji.200535549]

Fractalkine (CX3CL1) is a unique membrane-bound CX3C chemokine that serves as a potent chemoattractant for lymphocytes. The hypothesis of this study is that dendritic cells (DC) genetically modified *ex vivo* to overexpress fractalkine would enhance the T cell-mediated cellular immune response with a consequent induction of anti-tumor immunity to suppress tumor growth. To prove this hypothesis, established tumors of different mouse cancer cells (B16-F10 melanoma, H-2^b, and Colon-26 colon adenocarcinoma, H-2^d) were treated with intratumoral injection of bone marrow-derived DC that had been modified *in vitro* with an RGD fiber-mutant adenovirus vector expressing mouse fractalkine (Ad-FKN). In both tumor models tested, treatment of tumor-bearing mice with Ad-FKN-transduced DC gave rise to a significant suppression of tumor growth along with survival advantages in the treated mice. Immunohistochemical analysis of tumors treated with direct injection of Ad-FKN-transduced DC demonstrated that the treatment prompted $CD8^+$ T cells and $CD4^+$ T cells to accumulate in the tumor milieu, leading to activation of immune-relevant processes. Consistent with the finding, the intratumoral administration of Ad-FKN-transduced DC evoked tumor-specific cytotoxic T lymphocytes, which ensued from *in vivo* priming of Th1 immune responses in the treated host. In addition, the anti-tumor effect provided by intratumoral injection of Ad-FKN-transduced DC was completely abrogated in $CD4^+$ T cell-deficient mice as well as in $CD8^+$ T cell-deficient mice. These results support the concept that genetic modification of DC with a recombinant fractalkine adenovirus vector may be a useful strategy for cancer immunotherapy protocols.

Key words: Chemokines · Chemotaxis · Dendritic cells · Tumor immunity

Supporting information for this article is available at http://www.wiley-vch.de/contents/jc_2005/35549_s.pdf

Introduction

Dendritic cells (DC) are professional antigen-presenting cells, and possess an exquisite capacity to trigger the T cell activation required for the initiation and modulation of immune responses [1–3]. DC are strategically situated at the interface of potential pathogen entry sites to capture antigen [1, 2]. After the antigen uptake, they

* These authors contributed equally to this work.

Correspondence: Toshiaki Kikuchi, Department of Respiratory Oncology and Molecular Medicine, Institute of Development, Aging and Cancer, Tohoku University, 4–1 Seiryomachi, Aobaku, Sendai 980–8575, Japan
Fax: +81-22-717-8549
e-mail: kikuchi@idac.tohoku.ac.jp

Abbreviations: Ad-FKN: adenovirus vector expressing mouse fractalkine · **rFKN:** recombinant fractalkine

undergo maturation and move into secondary lymphoid organs to present the antigenic peptides to T lymphocytes [1, 2]. For efficient antigen presentation, the matured DC produce T cell-attracting chemokines that facilitate attracting T cells [4]. Fractalkine (CX3CL1) is a CX3C chemokine included in such T cell attractants expressed by mature DC [5–9]. Fractalkine has a unique membrane-bound structure with the chemokine domain perched atop a long mucin-like stalk at the cell surface, and can be cleaved by ADAM10 (ADAM for a disintegrin and metalloproteinase) or TNF-α-converting enzyme (TACE or ADAM17) to produce a soluble 80-kDa glycoprotein [5, 7, 10, 11]. The structure of fractalkine allows not only the shed soluble form to recruit T cells and monocytes expressing its specific receptor CX3CR1 in local chemoattractant gradients, but also the membrane-anchored form to act upon CX3CR1-positive cells directly and promote the cell-cell adhesion [5–7].

Although many tumors have antigens recognizable by the immune system, the escape of tumors from immunological surveillance suggests that the immune mechanism lacks something to overcome the growing potential of the tumors [12, 13]. In an attempt to provoke anti-tumor immunity efficiently, the present study focuses on a strategy to enhance the ability of DC to attract T lymphocytes for antigen presentation by the genetic strategy of modifying DC to express fractalkine. To accomplish this, we used an RGD fiber-mutant recombinant adenovirus vector expressing fractalkine (Ad-FKN) to transfer the mouse fractalkine cDNA to DC, and then injected the modified DC into established tumors. The data demonstrate that intratumoral injection of Ad-FKN-transduced DC elicits specific anti-tumor immunity, and inhibits the growth of established tumors, leading to improved survival of the tumor-bearing hosts.

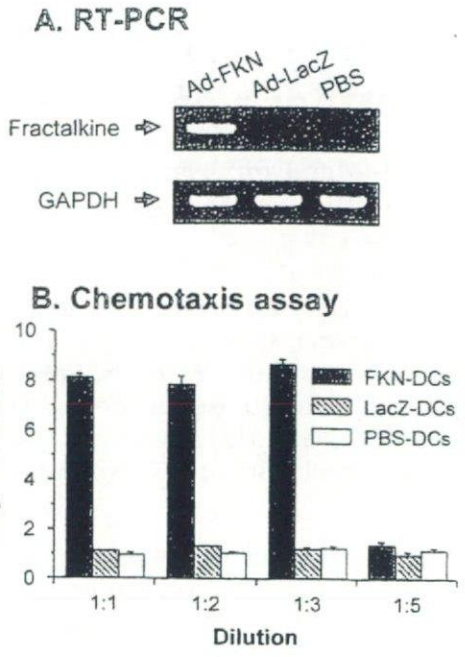

Figure 1. Fractalkine expression in genetically modified DC. (A) RT-PCR analysis for fractalkine mRNA expression. DC were transduced with Ad-FKN or Ad-LacZ at an MOI of 100 for 3 h, or PBS alone (mock transduction). After 48 h, total cellular RNA was extracted from the transduced cells, and reverse transcribed using oligo(dT) primer. The generated cDNA was used as a template to amplify fractalkine and GAPDH cDNA fragments by PCR. Samples were separated by 1% agarose gel electrophoresis and stained with ethidium bromide. (B) Chemotaxis assay using conditioned media of genetically modified DC. THP-1 cells placed in the upper chamber of a transwell chamber were assayed for chemotaxis in response to serial dilutions of supernatant from DC transduced with Ad-FKN or Ad-LacZ (MOI 100, 3 h), or PBS alone (mock transduction) in the lower chamber. The number of cells migrating to the lower chamber at 37°C for 4 h was counted by flow cytometric analysis. The migration index was calculated as the number of cells migrating to the conditioned media over the number of cells migrating to the control medium. Results represent the mean ± standard error (n=3 per data point).

Results

Ad-FKN modification of DC

To enhance the chemoattracting property of DC, we genetically modified DC with an RGD fiber-mutant recombinant adenovirus vector ($E1^-$) expressing mouse fractalkine (Ad-FKN), and confirmed the induced fractalkine expression of the modified DC by RT-PCR and chemotaxis assay (Fig. 1). In the RT-PCR analysis, 0.7-kb fragments corresponding to the fractalkine mRNA were markedly or slightly amplified with the total cellular RNA from Ad-FKN-transduced DC or Ad-LacZ-transduced DC, respectively, but were not amplified with that from non-transduced DC (Fig. 1A). Comparable levels of expression of the housekeeping GAPDH gene in all DC demonstrated the intactness of the RNA samples from the Ad-FKN-transduced and control Ad-LacZ-transduced DC as well as the non-transduced DC. The chemoattracting activity of the fractalkine produced by Ad-FKN-transduced DC was assayed using the THP-1 leukemia cell line (Fig. 1B). An eightfold migratory response of THP-1 cells was observed in the non-diluted culture supernatant of Ad-FKN-transduced DC compared with that of Ad-LacZ-transduced DC and non-transduced DC (1:1 dilution, $p<0.00001$). Similar results were achieved in the 1:2 and 1:3 dilutions (1:2 dilution, six- to sevenfold, $p<0.0001$; 1:3 dilution, sevenfold, $p<0.00001$; Ad-FKN-transduced DC compared with Ad-LacZ-transduced DC and non-transduced DC), although the chemoattracting potential of the supernatant of Ad-FKN-

transduced DC disappeared at the 1:5 dilution ($p>0.2$, Ad-FKN-transduced DC compared with all other control DC). There were no detectable differences in the chemoattracting function of the supernatant between Ad-LacZ-transduced DC and non-transduced DC at any dilutions ($p>0.05$). These results showed that the Ad-FKN infection of DC robustly enhanced the fractalkine mRNA expression, endowing the Ad-FKN-transduced DC with high chemoattracting activity, but that the control adenovirus vector (*i.e.*, Ad-LacZ) infection slightly increased the fractalkine mRNA expression without affecting the chemoattracting property. The relevance of the observed chemotaxis to adenovirus-mediated fractalkine expression was demonstrated by the observation that the chemotactic activities of the Ad-FKN-conditioned media and the recombinant fractalkine (rFKN) were significantly inhibited by an addition of neutralizing anti-mouse fractalkine antibody to the media (Ad-FKN-transduced DC, $p<0.0001$; rFKN, $p<0.005$), but unaffected by that of isotype-matched control antibody (Ad-FKN-transduced DC, $p>0.1$; rFKN, $p>0.6$; supplementary Fig. 1). No striking difference was observed between Ad-FKN- and non-transduced DC in the migratory ability to the draining lymph nodes (supplementary Fig. 2).

Anti-tumor effects of Ad-FKN-transduced DC

In B16-F10-bearing C57BL/6 mice (H-2^b), marked tumor suppression was observed with intratumoral administration of Ad-FKN-transduced DC, in contrast to that of Ad-LacZ- or non-transduced DC ($p<0.05$ at 11–17 days), and the treatment of Ad-FKN-transduced DC resulted in a survival advantage (Kaplan-Meier analysis, $p<0.05$ to all other groups; Fig. 2A). Administration of Ad-LacZ-transduced DC had no beneficial effect as compared to that of non-transduced DC (tumor size, $p>0.3$; survival, $p>0.5$; Fig. 2A). Similar results were achieved in the Colon-26 tumor model in BALB/c mice (H-2^d). Tumor growth was suppressed significantly by the treatment of Ad-FKN-transduced DC as compared to that of all other control DC (days 8–16, $p<0.05$), leading to long-term survival in 40% of the Ad-FKN-transduced DC-treated mice ($p<0.05$ to all other groups; Fig. 2B). Tumors injected with Ad-LacZ-transduced DC grew in a similar fashion to tumors treated with non-transduced DC ($p>0.05$) and did not have enhanced survival ($p>0.4$; Fig. 2B). The anti-tumor effect of Ad-FKN-transduced DC was also observed in the larger Colon-26 tumor model over days 16–20 ($p<0.05$ to all other groups; supplementary Fig. 3). In addition, the specificity of the anti-tumor effect produced by Ad-FKN-transduced DC was ascertained using Ad-FKN-transduced fibroblasts as a control (days 7–19, $p<0.05$ compared with control mice that had been treated with Ad-FKN-transduced fibroblasts and non-transduced DC; supplementary Fig. 4).

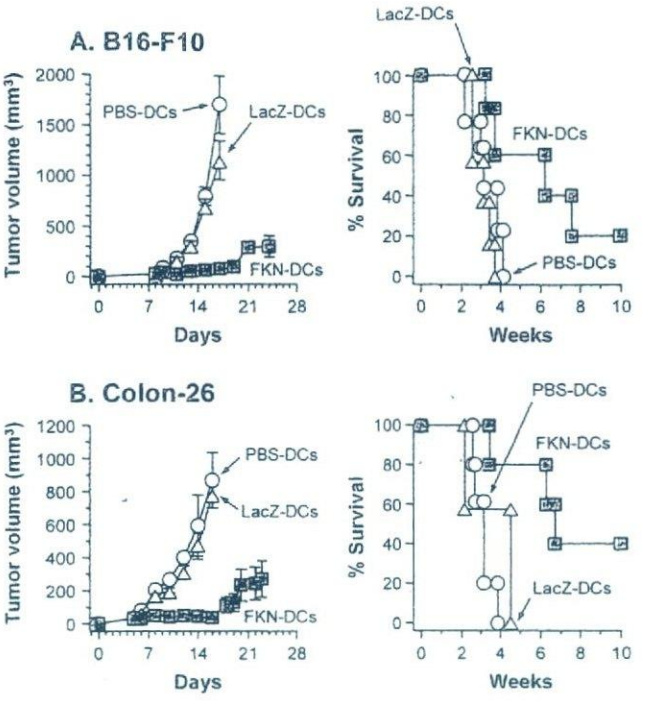

Figure 2. Tumor growth and survival of mice treated with intratumoral administration of Ad-FKN-modified DC. (A) B16-F10 tumors, C57BL/6 mice. B16-F10 cells (3×10^5) were implanted subcutaneously in the right flank of C57BL/6 mice (day 0). On day 8, tumor-baring mice were treated by intratumoral injection of 7×10^5 DC transduced with Ad-FKN (■), Ad-LacZ (△), or PBS alone (○). (B) Colon-26 tumors, BALB/c mice. This study is similar to that in (A), but BALB/c mice with 5-day established Colon-26 tumors were treated. For the left panels, the size of each tumor was assessed using calipers, and is reported as the average tumor volume (mm^3) ± standard error (n=5 per group). For the right panels, survival was recorded as the percentage of animals in each group.

Intratumoral T cell infiltration provoked by Ad-FKN-transduced DC

Fractalkine-expressing DC that had been injected into the established tumors augmented the intratumoral infiltration of both $CD4^+$ T cells and $CD8^+$ T cells (Fig. 3). Immunohistochemical analyses demonstrated an enhanced accumulation of $CD4^+$ T cells within Colon-26 tumors treated with Ad-FKN-transduced DC as compared to control tumors treated with Ad-LacZ- or non-transduced DC ($CD4^+$ T cells per ten random high-power fields: Ad-FKN-transduced DC 385, LacZ-DC 21, PBS-DC 34, Fig. 3A–C). Similar results were achieved for $CD8^+$ T cells. A markedly increased number of $CD8^+$ T cells accumulated in Colon-26 subcutaneous tumors treated with direct administration of Ad-FKN-trans-

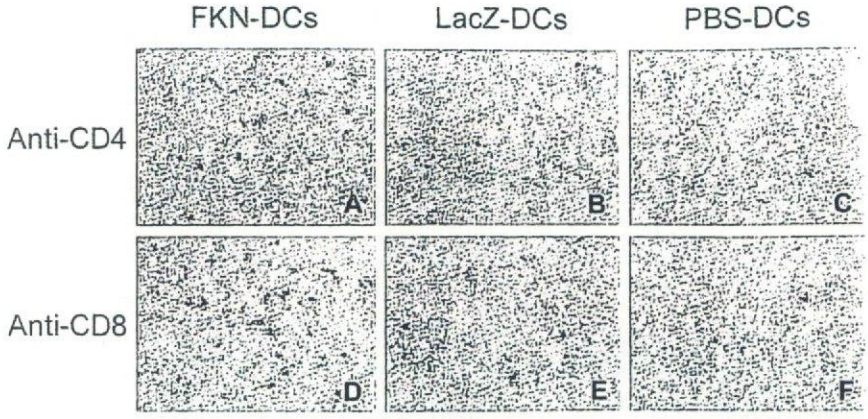

Figure 3. Immunohistochemical evaluation of tumors treated with Ad-FKN-modified DC. BALB/c mice with 5-day established subcutaneous Colon-26 tumors were treated by intratumoral injection of 7×10^5 DC that had been transduced with Ad-FKN (A, D), Ad-LacZ (B, E), or PBS (C, F). The tumors were dissected 3 days after the injection, and the frozen tumor sections were stained with anti-mouse CD4 antibodies (A–C) or anti-mouse CD8 antibodies (D–F). Signals were amplified by secondary biotinylated antibodies and detected by peroxidase-conjugated streptavidin and DAB. Nuclei of sections were counterstained with methyl green.

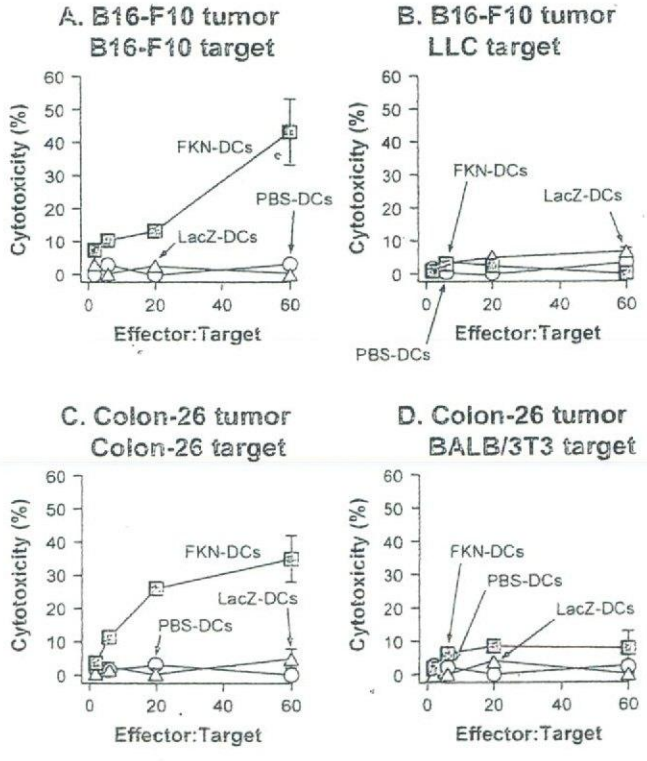

Figure 4. Induction of tumor-specific cytotoxic T cells by intratumoral injection of Ad-FKN-modified DC. (A, B) B16-F10 tumors. C57BL/6 mice bearing 8-day established subcutaneous B16-F10 tumors were treated by intratumoral injection of 7×10^5 DC transduced with Ad-FKN (▣), Ad-LacZ (△), or PBS (○). At 10 days after the treatment, spleen cells were isolated and restimulated with mitomycin C-treated B16-F10 for 5 days. The restimulated effector cells were then assayed for cytolytic function using B16-F10 cells (A) or LLC cells (B) as target cells. (C, D) Colon-26 tumors. This study was similar to that described in (A) and (B), but BALB/c mice with 5-day established Colon-26 tumors were treated. Colon-26 cells (C) or BALB/3T3 cells (D) were used as target cells. Results are shown as the mean ± standard error (n=3 per data point).

duced DC, but this was not observed in any other control tumors ($CD8^+$ T cells per ten random high-power fields: Ad-FKN-transduced DC 443, LacZ-DC 16, PBS-DC 23, Fig. 3D–F).

Anti-tumor CTL induced by intratumoral injection with Ad-FKN-transduced DC

Direct injection of Ad-FKN-transduced DC to B16-F10 or Colon-26 tumors elicited tumor-specific CTL activity (Fig. 4). C57BL/6 mice bearing B16-F10 tumors were intratumorally injected with Ad-FKN-, Ad-LacZ-, or non-transduced DC. Effector cells were generated from splenocytes obtained 10 days after the injection by culture with mitomycin C-treated B16-F10 cells. Effector cells from mice treated with Ad-FKN-transduced DC exhibited remarkable lysis of B16-F10 target cells, but control effector cells of mice treated with Ad-LacZ- or non-transduced DC exhibited minimal lysis (Fig. 4A). No apparent lysis was observed against irrelevant but syngenic LLC cells (Fig. 4B). BALB/c mice bearing Colon-26 tumors treated with Ad-FKN-transduced DC exhibited a strong Colon-26-specific splenic CTL response (Fig. 4C, D). Controls for this analysis included lymphocytes obtained from tumor-bearing mice injected with Ad-LacZ- or non-transduced DC. Splenocytes were restimulated with Colon-26 cells as described above, and the resulting effector cells were evaluated for cytolytic activity against Colon-26 and BALB/3T3 cells. Only Ad-FKN transduction markedly enhanced the cytolytic activity against Colon-26 cells. With effector cells in the Colon-26 tumor model, no lysis was observed against BALB/3T3 cells. The relevance of the *in vitro* tumor cytolysis to *in vivo* function was demonstrated by showing that BALB/c mice eradicating Colon-26 tumors after intratumoral administration of Ad-FKN-transduced

DC acquired resistance to the subsequent rechallenge of Colon-26 tumors ($p<0.000001$ to control mice; supplementary Fig. 5).

Splenic responses of mice treated with Ad-FKN-transduced DC

The treatment of Ad-FKN-transduced DC elicited cytokine-secreting reactivity in spleens of C57BL/6 mice bearing B16-F10 tumors (Fig. 5). B16-F10 tumors were treated by intratumoral inoculation of Ad-FKN-, Ad-LacZ-, or non-transduced DC, and splenocytes of the treated mice were evaluated for their IFN-γ- and IL-4-secreting reactivity against B16-F10 cells. The co-culture with the parental B16-F10 cells significantly induced IFN-γ release from the spleen cells of mice treated with Ad-FKN- and Ad-LacZ-transduced DC ($p<0.01$ compared with non-transduced DC), and the level of IFN-γ in the Ad-FKN/DC-treated group was 3.3-fold greater than that in the Ad-LacZ/DC-treated group ($p<0.0001$). On the other hand, the spleen cells from Ad-FKN-transduced DC-treated mice exhibited moderate enhancement of IL-4 production in the co-culture with B16-F10 cells ($p<0.0005$ compared with control spleen cells from mice that had been treated with Ad-LacZ- and non-transduced DC). No increase in the secretion of IL-4 was observed with splenocytes from mice treated with Ad-LacZ-transduced DC ($p>0.05$ compared with non-transduced DC).

Requirements of $CD4^+$ and $CD8^+$ T cells

To determine the role of $CD4^+$ T cells and $CD8^+$ T cells in the anti-tumor responses prompted by intratumoral administration of Ad-FKN-transduced DC, B16 tumors established in wild-type, $CD4^+$ T cell-deficient ($CD4^{-/-}$), or $CD8^+$ T cell-deficient ($CD8^{-/-}$) C57BL/6 mice were treated by intratumoral injection with Ad-FKN-transduced DC (Fig. 6). The growth of B16 tumors in $CD4^{-/-}$ and $CD8^{-/-}$ mice was not abated by the Ad-FKN-transduced DC treatment compared with that in wild-type mice receiving the identical treatment, and it was similar to the growth of PBS-treated B16 tumors in wild-type mice (days 10–18, $p<0.05$, $CD4^{-/-}$ and $CD8^{-/-}$ mice compared with Ad-FKN-transduced DC-treated wild-type mice; $p>0.05$ or $p>0.05$, $CD4^{-/-}$ or $CD8^{-/-}$ mice compared with PBS-treated wild-type mice, respectively; Fig. 6).

Discussion

In the present study, we hypothesized that genetic modification of DC with an RGD fiber-mutant recombinant adenovirus to express a T lymphocyte chemoattractant, fractalkine, would enable them to attract T lymphocytes for optimal antigen presentation, and to initiate tumor-specific cellular immune responses for suppressing the tumor growth. The data support this hypothesis. Intratumoral administration of Ad-FKN-transduced DC to two different types of mouse tumors elicited therapeutic anti-tumor immunity that suppressed the growth of established tumors and increased the survival of the tumor-bearing hosts. The observed tumor suppression was coupled with the induction of tumor-specific CTL *in vivo*, and the involvement of Th1-dominant immune responses was suggested by the cytokine analyses. In line with the immunohistochem-

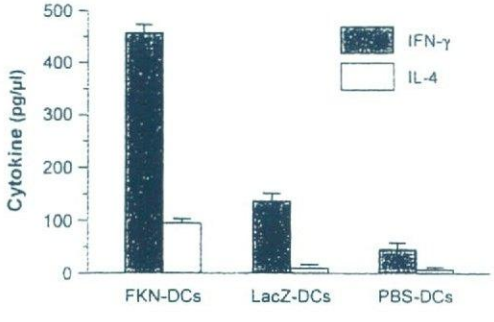

Figure 5. Cytokine profile of splenocytes from tumor-bearing mice treated by intratumoral injection of Ad-FKN-modified DC. C57BL/6 mice bearing 8-day established subcutaneous B16-F10 tumors were treated by intratumoral injection of 7×10^5 DC transduced with Ad-FKN (FKN-DC), Ad-LacZ (LacZ-DC), or PBS (PBS-DC). At 10 days after the treatment, spleen cells were isolated and co-cultured for 5 days with mitomycin C-treated B16-F10 in 24-well culture plates. The culture medium was collected, and the levels of mouse IFN-γ and IL-4 were assayed by ELISA. Results are shown as the mean ± standard error (n=3 per data point).

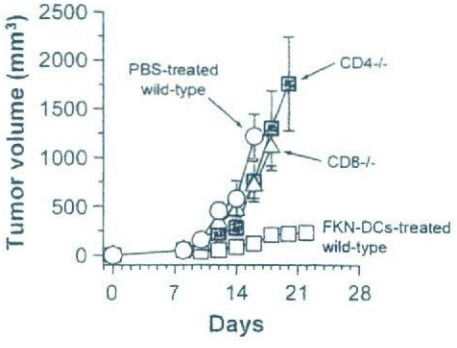

Figure 6. The role of $CD4^+$ and $CD8^+$ T cells in suppressing tumor growth by intratumoral injection of Ad-FKN-modified DC. $CD4^+$ T cell-deficient (■), $CD8^+$ T cell-deficient (△), or wild-type C57BL/6 mice (□) bearing 8-day established subcutaneous B16-F10 tumors were treated by intratumoral injection of 7×10^5 DC transduced with Ad-FKN. The size of each tumor was assessed using calipers, and is reported as the average tumor volume (mm^3) ± standard error (n=5 per group). Controls included tumor-bearing wild-type C57BL/6 mice that had been treated by intratumoral injection of PBS alone (○).

ical evidence that both $CD4^+$ T cells and $CD8^+$ T cells accumulated in the Ad-FKN-transduced DC-treated tumors, the knockout mice experiments demonstrated that both $CD4^+$ T cells and $CD8^+$ T cells are required for the therapeutic efficacy of Ad-FKN-transduced DC administered to established tumors.

The observations in the present study are consistent with the concept that DC transduced to express fractalkine efficiently initiate protective anti-tumor immunity. DC are professional antigen-presenting cells that take up antigens in peripheral tissues and migrate to lymphoid organs where they present antigens to T lymphocytes [1–3]. Several reports suggest that, in many instances, DC cannot stimulate cytotoxic $CD8^+$ T cells directly unless they contact activated $CD4^+$ T cells and are stimulated by multiple ligand-receptor pairs such as CD40 on DC and CD40 ligand on activated $CD4^+$ T cells [14]. In this context, DC present antigenic peptides associated with MHC class II molecules to $CD4^+$ helper T cells, and drive their proliferation and differentiation [1–4, 15]. Therefore, the direct interaction of DC and T cells is of central importance in priming specific immune responses [4, 15–17]. This is achieved not only by the DC migrating to the T cell-rich area of lymphoid organs, but also by the DC themselves producing chemokines that stimulate DC-T cell interaction [4, 18]. Fractalkine is one of such T cell-attracting chemokines, and has recently been shown *in vitro* and *in vivo* to attract subsets of activated T cells, in particular Th1 $CD4^+$ T cells [19]. These observations suggest that fractalkine may further enhance the encounter of antigen-specific T cells with antigen-bearing DC, and thus retain the DC-T cell interactions for prolonged periods of time to achieve the T cell activation [15, 17, 18]. In keeping with this knowledge, the present study has demonstrated that genetic modification of DC to express fractalkine accomplishes the goal of optimal DC-T cell interaction to induce functionally relevant cell-mediated adaptive immune responses, such as the suppression of tumor growth in an antigen-specific fashion. When administered to tumors, DC which have been modified with Ad-FKN most likely capture tumor antigens, and present processed protein antigens of tumor origin on MHC class II molecules. Adenovirus vector-mediated fractalkine probably enhanced the extent of the encounter between antigen-presenting DC and antigen-specific $CD4^+$ T cells, thus more efficiently amplifying the relevant antigen-specific immune responses. Consistent with this hypothesis, the administration of fractalkine-transduced DC to tumors resulted in the local accumulation of both $CD4^+$ T cells and $CD8^+$ T cells. Further evidence for this concept comes from the observations that the Ad-FKN-transduced DC treatment could not induce the tumor regression in either $CD4^+$ T cell-deficient mice or $CD8^+$ T cell-deficient mice, and that the intratumoral administration of Ad-FKN-transduced DC elicited IFN-γ-secreting reactivity in spleens of the tumor-bearing mice.

Based on the chemoattractive and promotive effects of chemokines on different leukocyte subpopulations *in vitro* and *in vivo*, a variety of strategies for cancer immunotherapy have been developed: the transduction of tumor cells with chemokine genes, the injection of recombinant chemokine protein into tumor sites, the administration of fusion proteins combining tumor antigen and chemokine, and the transfection of chemokine genes into DC or stromal cells [20–22]. Studies with experimental tumor models have shown that the introduction of chemokines including T cell activation protein-3 (TCA-3; CCL1), monocyte chemoattractant protein-1 (MCP-1; CCL2), macrophage inflammatory protein-1α (MIP-1α; CCL3), regulated on activation normal T cell expressed and secreted (RANTES; CCL5), hemofiltrate CC chemokine-4 (HCC-4; CCL16), macrophage inflammatory protein-3β (MIP-3β; CCL19), macrophage inflammatory protein-3α (MIP-3α; CCL20), secondary lymphoid tissue chemokine (SLC; CCL21), macrophage-derived chemokine (MDC; CCL22), interleukin-11 receptor α-locus chemokine (ILC; CCL27), fractalkine (CX3CL1), monokine induced by γ-interferon (Mig; CXCL9), γ-interferon-inducible protein-10 (γIP-10; CXCL10), and lymphotactin (XCL1), is capable of inducing anti-tumor immunity resulting in tumor regression [21, 23–27].

Several chemokine gene modifications of DC have been evaluated in an attempt to stimulate tumor-specific cellular immunity through the preferential attraction of T lymphocytes [22]. Cao *et al.* [28] reported that immunization with lymphotactin gene-modified DC pulsed with 3LL cell-specific Mut1 peptide induced specific CTL responses against 3LL tumor cells, and could render mice completely resistant to 3LL tumor cell challenge. Kirk *et al.* [29] showed that the anti-tumor response mediated by DC pulsed with tumor lysate in a distal immunization site of tumor-bearing mice could be improved by genetically modifying the DC to express SLC. Yang *et al.* [30] also used DC genetically modified *ex vivo* to express SLC to induce anti-tumor immunity in a mouse tumor model. Finally, Matsuyoshi *et al.* [31] compared the anti-tumor effect of DC modified to express limphotactin, SLC, and Mig, and observed that, among the three types of chemokine gene-modified DC, SLC-expressing DC were the most potent in priming tumor-specific CTL *in vivo* and providing the immunized mice with protection against subsequent tumor challenge. The present study has extended the concept of using chemokine gene-modified DC to induce the formation of the immunological synapse that determines the class of immune response, and demonstrated that genetic modification of DC to express fractalkine, a

CX3C chemokine that preferentially attracts Th1 cells, enhances their capacity to elicit a Th1-poralized anti-tumor immunity.

Materials and methods

Mice

Female C57BL/6 (H-2^b) and BALB/c (H-2^d) mice, 6–10 weeks old, were purchased from Japan Charles River (Atsugi, Japan). $CD4^+$ T cell-deficient (B6.129S2-*Cd4*^{tm1Mak}) and $CD8^+$ T cell-deficient (B6.129S2-*Cd8a*^{tm1Mak}) mice that had been back-crossed to the C57BL/6 background were obtained from Jackson Laboratory (Bar Harbor, ME). Animals were housed under specific pathogen-free conditions in accordance with the guidelines of the institutional Animal Care and Use Committee.

Cell culture

The Colon-26 colon adenocarcinoma cell line (H-2^d), the BALB/3T3 fibroblast cell line (H-2^d), the B16-F10 melanoma cell line (H-2^b), the Lewis lung carcinoma (LLC) cell line (H-2^b), and the THP-1 human monocytic leukemia cell line were obtained from the Cell Resource Center for Biomedical Research (Tohoku University, Sendai, Japan). The LLC cell line was maintained in complete Dulbecco's modified Eagle's media (10% FBS, 100 μg/mL streptomycin, and 100 U/mL penicillin). All other cell lines were maintained in complete RPMI 1640 media. DC were generated from mouse bone marrow precursors in complete RPMI 1640 media with 10 ng/mL recombinant mouse granulocyte-macrophage colony-stimulating factor (GM-CSF; R&D Systems Inc., Minneapolis, MN) and 2 ng/mL recombinant mouse IL-4 (R&D Systems), as described previously [32–34].

Adenovirus vectors

The replication-deficient adenovirus vectors with an RGD fiber mutation used in this study are based on the human Ad5 genome with E1 and E3 deletions. The Ad-FKN vector and the Ad-LacZ control vectors express the mouse fractalkine cDNA and the lacZ cDNA, respectively, under the control of the cytomegalovirus early/immediate promoter/enhancer. The propagation, purification and titration of the adenovirus vectors were as previously described [35]. All vectors were free of replication competent adenovirus.

RT-PCR

Total cellular RNA was extracted from the cells using ISOGEN (Nippon Gene Co., Tokyo, Japan), and 2 μg RNA were subjected to reverse transcription using the RNA PCR kit (Takara Shuzo Co., Kyoto, Japan) at 42°C in a total volume of 20 μL. One tenth of the cDNA was amplified with the following primers specific for either fractalkine or the control glyceraldehyde-3-phosphate dehydrogenase (GAPDH) transcripts: for fractalkine, 5′-GCTTACGGCTAAGCCTCAGA-3′ and 5′-CACTGGCACCAGGACGTATG-3′; for GAPDH, 5′-ATGGTGAAGGTCGGTGTGAACGGA-3′ and 5′-TTACTCCTTGGAGGCCATGTAGGC-3′. The amplification profile was 94°C for 2 min, 36 cycles of 94°C for 30 s, 60°C for 30 s, and 72°C for 90 s. One tenth of the PCR product was resolved on a 1% agarose gel and stained with 0.5 μg/mL ethidium bromide.

Chemotaxis assay

To determine the function of the fractalkine protein produced by the Ad-FKN-transduced DC, the supernatant of the genetically modified DC was obtained from the culture in RPMI 1640 medium containing 1% FBS, and serial dilutions (1:1, 1:2, 1:3 and 1:5) were placed in the lower chambers of 5-μm pore transwell plates (Corning Costar Inc., Corning, NY). THP-1 cells (10^5 cells) suspended in RPMI 1640 medium containing 1% FBS were loaded to the upper chambers, and incubated for 3 h at 37°C. The number of migrating cells into the lower chamber was determined by flow cytometric analysis. The migration index was calculated as the number of cells migrating into the conditioned medium divided by the number of cells migrating into the control medium alone.

Tumor therapy model

B16-F10 cells (3×10^5) or Colon-26 cells (2×10^5) were injected subcutaneously into the right flank of C57BL/6 mice or BALB/c mice, respectively. When the tumors had grown and could be easily palpated (day 8 for B16-F10 tumors; day 5 for Colon-26 tumors), they were injected with 7×10^5 DC that had been transduced with Ad-FKN, Ad-LacZ, or PBS alone (*i.e.*, mock transduction) at a MOI of 100 for 3 h. The size of each tumor was assessed using calipers, and was recorded as the tumor volume (length × width^2 × 0.52). When animals became moribund or the tumors reached 20 mm in diameter, the mice were killed, and this was recorded as the date of death for the survival studies. Where indicated, $CD4^+$ T cell-deficient mice and $CD8^+$ T cell-deficient mice were used for the B16-F10 tumor model.

Immunohistochemistry

Three days after the treatment of tumor-bearing BALB/c mice (intratumoral injection of the genetically modified DC to 5-day established subcutaneous Colon-26 tumors), the tumors were removed, and frozen sections of 5 μm in thickness were prepared and fixed in acetone. After blocking nonspecific staining and endogenous peroxidase, sections were incubated with 0.31 μg/mL anti-mouse CD4 mAb (clone RM4–5; BD Bioscience PharMingen) or 10 μg/mL anti-mouse CD8 mAb (clone KT15; Serotec, Kidlington, UK) overnight at 4°C [36]. After washing, the specimens were then incubated with 2.5 μg/mL biotinylated rabbit anti-rat immunoglobulins (DakoCytomation, Glostrup, Denmark) for 15 min at room temperature. Signals were visualized with horseradish peroxidase-conjugated streptavidin and 3–3′-diaminobenzidine tetrahydrochloride (DAB) chromogen/substrate mixture (Nichirei, Tokyo, Japan). The sections were then incubated with 2.5% methyl green for nuclear counterstaining [36].